

1 **Late Paleocene – middle Eocene benthic foraminifera on a Pacific Seamount**
2 **(Allison Guyot, ODP Site 865): Greenhouse Climate and superimposed**
3 **hyperthermal events**

4
5 Arreguín-Rodríguez, G. J., Alegret, L., Thomas, E.

6
7 Gabriela J. Arreguín-Rodríguez, Departamento de Ciencias de la Tierra, Universidad de
8 Zaragoza, Pedro Cerbuna 12, 50009, Zaragoza, Spain.

9 Laia Alegret, Departamento de Ciencias de la Tierra, Universidad de Zaragoza, Pedro
10 Cerbuna 12, 50009, Zaragoza, Spain, and Instituto Universitario de Ciencias
11 Ambientales, Universidad de Zaragoza, Zaragoza, Spain.

12 Ellen Thomas, Department of Geology and Geophysics, Yale University, New Haven
13 CT, USA, and Department of Earth and Environmental Sciences, Wesleyan
14 University, Middletown CT, USA.

15 Corresponding author: Gabriela J. Arreguín-Rodríguez (Tel: +34 976761079. E-mail:
16 arreguin@unizar.es)

17
18
19
20
21
22
23
24
25

26 **Key points:**

- 27 - Seamount-assemblages dominated by shallow-infaunal suspension feeders
- 28 - Post-PETM faunas affected by ocean acidification and changes in current regime
- 29 - PETM and ETM3 associated with increased food supply through trophic
- 30 focusing

31

32 **Abstract**

33 We investigated the response of late Paleocene-middle Eocene (~60-37.5 Ma)
34 benthic foraminiferal assemblages to long term climate change and hyperthermal events
35 including the Paleocene-Eocene Thermal Maximum (PETM) at ODP Site 865 on
36 Allison Guyot, a seamount in the Mid-Pacific Mountains. Seamounts are isolated deep-
37 sea environments where enhanced current systems interrupt benthic-pelagic coupling,
38 and fossil assemblages from such settings have been little evaluated. Assemblages at
39 Site 865 are diverse and dominated by cylindrical calcareous taxa with complex
40 apertures, an extinct group which probably lived infaunally. Dominance of an infaunal
41 morphogroup is unexpected in a highly oligotrophic setting, but these forms may have
42 been shallow infaunal suspension feeders, which were ecologically successful on the
43 current-swept seamount. The magnitude of the PETM extinction at Site 865 was similar
44 to other sites globally, with lower diversity post-extinction faunas affected by ocean
45 acidification and changes in current regime, which might have led to increased nutrient
46 supply through trophic focusing. A minor hyperthermal (ETM3) saw less severe effects
47 of changes in current regime, with no evidence for carbonate dissolution. Although the
48 relative abundance of infaunal benthic foraminifera has been used as a proxy for surface
49 productivity through benthic-pelagic coupling, we argue that this proxy can be used only
50 in the absence of changes in carbonate saturation and current-driven biophysical linking.

51

52 **Keywords:** benthic foraminifera, seamounts, hyperthermal events, currents,
53 acidification.

54

55 **1. Introduction**

56 The late Paleocene through early Eocene greenhouse world started to warm in
57 the late Paleocene, culminating the warmest part of the Cenozoic during the Early
58 Eocene Climate Optimum (EECO), followed by gradual cooling of high latitudes and
59 deep sea waters from the end of the early Eocene on [Zachos *et al.*, 2001, 2008]. This
60 long-term evolution was punctuated by short, extreme warming events called
61 hyperthermals [Thomas *et al.*, 2000; Thomas and Zachos, 2000; Cramer *et al.*, 2003;
62 Zachos *et al.*, 2010; Leon-Rodriguez and Dickens, 2010; Littler *et al.*, 2014]. During
63 such events, large amounts of isotopically light carbon were released rapidly into the
64 ocean-atmosphere system [Dickens *et al.*, 1995, 1997], causing negative carbon isotope
65 excursions (CIEs) in carbonate and organic matter, coeval with oxygen isotope
66 excursions indicative of warming, and dissolution of calcium carbonate [Cramer *et al.*,
67 2003; Zachos *et al.*, 2010].

68 The Paleocene-Eocene Thermal Maximum (PETM, ~55.5 Ma) was the most
69 extreme of these hyperthermals, characterized by a 5-8 °C increase in global
70 temperatures [Zachos *et al.*, 2003; Sluijs *et al.*, 2007; McInerney and Wing, 2011;
71 Dunkley Jones *et al.*, 2013], a negative CIE of at least ~2.5‰ and possibly up to 4.5‰
72 [Kennett and Stott, 1991; Thomas and Shackleton, 1996; McCarren *et al.*, 2008;
73 Handley *et al.*, 2008], ocean acidification of the surface ocean [e.g., Penman *et al.*,
74 2014], shoaling of the calcite compensation depth (CCD) and carbonate dissolution on
75 the seafloor [Zachos *et al.*, 2005], perturbation of the hydrological cycle [Pagani *et al.*,
76 2006; Eldrett *et al.*, 2014], and possibly regional deoxygenation of sea-bottom waters

77 [Chun *et al.*, 2010; Pälike *et al.*, 2014] and expanding Oxygen Minimum Zones [Zhou
78 *et al.*, 2014]. Carbon cycling within the oceans, specifically the depth of
79 remineralization of organic matter, may have changed during the warming [Ma *et al.*,
80 2014; John *et al.*, 2013, 2014], and open-ocean productivity may have declined [e.g.,
81 Winguth *et al.*, 2012]. Perturbation of biotic assemblages on land and in the oceans
82 [McInerney and Wing, 2011], including the largest extinction of deep-sea benthic
83 foraminifera of the Cenozoic [Thomas, 2007], are among the consequences of the
84 PETM, as are migrations of biota to higher latitudes on land and in the oceans [e.g.
85 McInerney and Wing, 2011; Speijer *et al.*, 2012]. Other hyperthermals, similar to the
86 PETM but of lesser magnitude, are less well documented (Table 1). In addition, at ~40
87 Ma the middle Eocene Climate Optimum (MECO) interrupted the deep-water and high-
88 latitude cooling trend starting at the end of the early Eocene [Bohaty and Zachos, 2003;
89 Bohaty *et al.*, 2009]. The MECO had a longer duration than earlier hyperthermals, with
90 peak warming not clearly associated with a CIE [Bohaty *et al.*, 2009; Sluijs *et al.*, 2013;
91 Boscolo-Galazzo *et al.*, 2014].

92 Many hyperthermals have been described only by fluctuations in proxies for
93 temperature using $\delta^{18}\text{O}$, carbonate/terrigenous content or $\delta^{13}\text{C}$ in bulk carbonates or
94 benthic foraminifera, and their occurrence at orbital frequencies highlighted [de Conto
95 *et al.*, 2012; Payros *et al.*, 2012; Littler *et al.*, 2014; Lauretano *et al.*, 2015], although
96 the PETM has been suggested to be out of phase with other hyperthermals [Cramer *et*
97 *al.*, 2003; Zachos *et al.*, 2010]. Biotic effects of other hyperthermals, such as the Eocene
98 Thermal Maximum 2 (ETM2) or Eocene Thermal Maximum 3 (ETM3) have been
99 described in much less detail and from fewer localities than the PETM [e.g. Agnini *et*
100 *al.*, 2009; d'Haenens *et al.*, 2012; Jennions *et al.*, 2015]. As an example, the deep-sea
101 benthic foraminiferal turnover across the PETM has been intensely studied over the past

102 decades [e.g., *Thomas*, 1998, 2003, 2007; *Alegret et al.*, 2009a, b, 2010], but there are
103 few studies dealing with the turnover across the ETM2 [*d'Haenens et al.*, 2012;
104 *Jennions et al.*, 2015] and the ETM3 [*Röhl et al.*, 2005], and they are all based on sites
105 in the Atlantic Ocean. Therefore, the characteristics of the various Eocene
106 hyperthermals and specifically their effects on the biota are not well known yet, but they
107 share features with the PETM such as global warming, negative CIEs, carbonate
108 dissolution, biotic perturbations and increased continental weathering [e.g., *Thomas and*
109 *Zachos*, 2000; *Nicolo et al.*, 2007; *Stap et al.*, 2010; *Lauretano et al.*, 2015].

110 Because of the similarities among the hyperthermals, it is widely accepted that
111 they may have had a common cause, i.e., emission of isotopically light carbon
112 compounds to the ocean-atmosphere system. The source of the carbon compounds as
113 well as the triggering mechanism of emission is still under strong debate, including such
114 diverse proposed sources as methane from dissociation of gas hydrates through oceanic
115 warming [e.g., *Dickens et al.*, 1995; *Dickens*, 2011] possibly triggered through orbital
116 forcing [*Lunt et al.*, 2011], release of carbon from organic matter oxidation through
117 drying of marginal basins [*Higgins and Schrag*, 2006], burning of peat deposits [*Kurtz*
118 *et al.*, 2003], heating of organic matter by intrusion of volcanic sills [*Svensen et al.*,
119 2004, 2010; *Storey et al.*, 2007], release of dissolved methane from a silled North
120 Atlantic basin [*Nisbet et al.*, 2009], and orbitally forced dissociation of permafrost
121 deposits on Antarctica [*de Conto et al.*, 2012].

122 Seamounts are geographically isolated topographic features rising > 100 m
123 above the surrounding seafloor [*Staudigel et al.*, 2010], where interaction of geological,
124 oceanographic and biological factors [*Genin*, 2004] creates unusual ecological settings,
125 commonly characterized by high biodiversity [*McClain*, 2007; *Shank*, 2010]. Because
126 of their geographic isolation, some authors consider the occurrence of endemic species

127 typical [e.g. *de Forges et al.*, 2000], whereas others argue that the observed percentage
128 of endemism may be biased by sampling problems [*McClain*, 2007; *McClain et al.*,
129 2009], or that the interaction of currents does not affect the efficiency of larval
130 dispersion [*Samadi et al.*, 2006]. Benthic foraminifera are characterized by a motile life
131 stage (propagules) [*Alve and Goldstein*, 2003, 2010], and genetic information on a few
132 deep-sea species suggests that they are cosmopolitan [*Pawlowski et al.*, 2007; *Burkett et*
133 *al.*, 2015], thus highly efficient dispersers. Studies on recent assemblages from
134 seamounts have not documented endemic benthic foraminiferal species [e.g. *Heinz et*
135 *al.*, 2004], although abyssal species inhabiting elevated objects on the seafloor appear to
136 differ between ocean basins [*Gooday et al.*, 2015].

137 Around the steep, abrupt seamount topography, currents are intensified,
138 including eddies and circular currents around the upper part of the seamount [*Lavelle*
139 *and Mohn*, 2010]. These currents winnow fine particles including organic matter, thus
140 removing food from benthic communities [e.g., *Heinz et al.*, 2004], but also trap
141 organisms and food particles in some parts of the seamount in a process called ‘trophic
142 focusing’, resulting in rich, sometimes highly localized concentrations of biota [*Genin*
143 *et al.*, 1998, *Genin*, 2004]. Importantly, effects of the current activity (biophysical
144 coupling) [*Dower and Brodeur*, 2004] around seamounts may break the link between
145 primary productivity in surface waters and arrival of food on the sea floor (bentho-
146 pelagic coupling). Food particles may be either swept away or concentrated, dependent
147 upon location on the seamount top, so that locally more or less food arrives at the
148 seafloor than calculated from primary productivity through application of a logarithmic
149 transfer equation [e.g., *Martin et al.*, 1987]. A seamount setting thus adds additional
150 complexity to the process of transfer of organic matter to the seafloor, a process now
151 realized to be much more complex than envisaged in the 1990s, with the transfer

152 equation highly dependent upon pelagic ecosystem structure [*Boyd and Trull, 2007;*
153 *Henson et al., 2012*]. In addition, transfer efficiency may vary during periods of climate
154 change, as a consequence of differentially changing metabolic rates of different
155 participants of the food chain [*Ma et al., 2014; John et al., 2013; 2014*].

156 Seamount-top ecosystems are commonly dominated by suspension feeders [e.g.,
157 *Genin et al., 1998*]. Meiofauna (including benthic foraminifera) may be reworked on the
158 top of the seamount [*Thistle et al., 1999; Wilson and Boehlert, 2004*], and strong near-
159 bottom flow may result in reduced abundance [*Thistle and Levin, 1998*]. The few
160 studies on seamount foraminifera suggest that their distribution and diversity are indeed
161 dominantly controlled by currents [*Kustanowich, 1962; Nienstedt and Arnold, 1988;*
162 *Ohkushi and Natori, 2001; Heinz et al., 2004; García-Muñoz et al., 2012*], whereas food
163 supply linked to primary productivity is generally seen as the main determinant of deep-
164 sea benthic foraminiferal faunas, when oxygen availability is not a critical factor [e.g.
165 *Jorissen et al., 1995; 2007*].

166 In order to compare the biotic turnover across the PETM and less intense
167 hyperthermal events at a location distal from the Atlantic Ocean, we document the long-
168 term, late Paleocene to middle Eocene evolution of benthic foraminifera on a seamount
169 in the Mid Pacific mountain chain, and evaluate the effects of long-term climate change
170 and superimposed, short-term hyperthermal events in this unusual setting.

171

172 **2. Setting of Site 865**

173 Paleocene-middle Eocene pelagic sediments overlying the top of Allison Guyot
174 in the equatorial Pacific (18°26' N, 179°33' W, 1530 m present water depth; Figure 1)
175 were recovered during Ocean Drilling Program Leg 143 at Site 865. We studied Cores
176 865B-3H to 865B-15X (upper Paleocene and Eocene), and included material from Core

177 865C-12H (uppermost Paleocene) because the PETM occurred in a core break
178 [*Bralower et al.*, 1995a, b]. These cores were recovered by hydraulic piston corer, with
179 the exception of Core 865B-15X, recovered with the Extended Core Barrel (XCB). The
180 correlation between cores from the two holes follows *Bralower et al.* [1995a, b].

181 The studied interval consists of about 116 m of pale yellow-white foraminiferal-
182 nannofossil ooze with burrow mottles with nannofossil ooze infill, and sporadic small
183 black specks towards the base of the studied interval. The carbonate content is
184 uniformly high, between 92 to 98% [*Sager et al.*, 1993]. Planktonic foraminifera, the
185 main component of the sand-size fraction, are strongly enriched over finer particles
186 through winnowing by bottom currents [*Sager et al.*, 1993; *Bralower et al.*, 1995a], as
187 seen in the high values of weight % of coarse fraction (CF; >63 μm) [*Yamaguchi and*
188 *Norris*, 2015]. Cores 865B-1H through the middle part of 865B-3H (present depth ~0-
189 19.2 mbsf) contain strongly mixed material from various ages, including Neogene and
190 Paleogene species, thus were excluded from this study [*Bralower et al.*, 1995a].

191 Below this interval, the record is almost complete for the time between about 60
192 and 38.5 Ma (upper Paleocene-middle Eocene), except for an unconformity over the
193 interval corresponding to ~49-51.5 Ma (present depth ~79.20-80.70 mbsf). The record
194 across the peak-PETM is condensed [*Bralower et al.*, 1995a, b; *Kelly et al.*, 1996, 1998;
195 *Nunes and Norris*, 2006], and there is considerable evidence for sediment mixing
196 through bioturbation and/or coring disturbance, as seen in the $\delta^{13}\text{C}$ signature of single
197 specimens of planktic foraminifera [e.g., *Kelly et al.*, 1996, 1998]. The paleodepth of
198 Site 865 was estimated as upper lower bathyal (~1300-1500 m), and it was at a
199 paleolatitude ranging from about 2°N in the Paleocene to 6°N in the late Eocene
200 [*Bralower et al.*, 1995a]. Calcareous nannofossil biostratigraphy was evaluated by
201 *Bralower and Mutterlose* [1995]. Planktic foraminifera underwent rapid evolution

202 across the PETM, with the so-called ‘excursion taxa’ (e.g. *Morozovella allisonensis*, *M.*
203 *africana* and *Acarinina sibaiyaensis*) indicating changes in water column stratification
204 and declining productivity, the latter supported by nanofossil evidence for intensified
205 oligotrophy in an already oligotrophic setting [Kelly *et al.*, 1996, 1998]. I/Ca values of
206 planktic foraminifera confirm that Site 865 was strongly oligotrophic [Zhou *et al.*,
207 2014]. Benthic ostracodes were studied at low resolution by *Boomer and Whatley*
208 [1995], in more detail by *Yamaguchi and Norris* [2015], showing significant extinction.
209 In contrast to the planktic records [Kelly *et al.*, 1996], benthic foraminiferal assemblages
210 have been interpreted as reflecting increased arrival of food at the seafloor [Thomas,
211 1998; Thomas *et al.*, 2000].

212 Planktic and benthic foraminiferal stable isotope stratigraphy was documented
213 by *Bralower et al.* [1995a, b], with additional benthic stable isotope data included in
214 *Thomas et al.* [2000] and *Katz et al.* [2003]. The long-term planktic and benthic
215 foraminiferal oxygen isotope records [Bralower *et al.*, 1995a, b] show an increase from
216 the end of the early Eocene on, interpreted as reflecting global cooling at this low
217 latitude site. Later evaluation documented extensive recrystallization of the planktic
218 foraminifera on the seafloor [Pearson *et al.*, 2001], indicating that high latitudes and
219 deep waters cooled, while tropical temperatures remained high [Pearson *et al.*, 2007].

220 Mg/Ca data on benthic foraminiferal tests across the PETM show bottom water
221 warming of about 3-4°C [Tripathi and Elderfield, 2005]. Stable isotope ($\delta^{18}\text{O}$) data for
222 planktic foraminifera across the PETM were interpreted to indicate minor surface water
223 warming [Bralower *et al.*, 1995 a, b], but later recognized to have been affected by
224 diagenesis on the sea floor [Pearson *et al.*, 2001; Kozdon *et al.*, 2011, 2013; Dunkley-
225 Jones *et al.*, 2013; Edgar *et al.*, 2015]. Detailed analysis of non-recrystallized parts of

226 the planktic tests indicates that sea surface temperatures (SST) increased by about 5°C
227 or more during the PETM, reaching at least 33°C [Kozdon *et al.*, 2011, 2013].

228 Diagenetic effects were more severe within the PETM interval, supporting the
229 occurrence of carbonate dissolution followed by reprecipitation, as suggested by the
230 presence of large euhedral calcite crystals encompassing planktic foraminifera [Kozdon
231 *et al.*, 2013] (Figure S1). Due to the lack of fine-grained terrestrial material, CaCO₃
232 dissolution during the PETM may not have resulted in formation of a clay layer, and
233 CaCO₃ wt % remained high in the interval with dissolution/reprecipitation across the
234 PETM. The observation that dissolution-recrystallization occurred during the PETM
235 but not at other intervals indicates that the lysocline was shallower than the paleodepth
236 of Site 865, even though carbonate dissolution was less severe in the Pacific than in the
237 Southeast Atlantic [Colosimo *et al.*, 2005; Zachos *et al.*, 2005].

238 Despite the problems in the stable isotope record of Site 865, negative $\delta^{13}\text{C}$
239 excursions mark the PETM and ETM3 [Bralower *et al.*, 1995a; Thomas *et al.*, 2000;
240 Zachos *et al.*, 2001]. Neither the ETM2 nor the MECO were recognized in the stable
241 isotope records at the resolution of our study, probably because of bioturbation and
242 coring disturbance combined with low sedimentation rates.

243 The main aspects of the benthic foraminiferal turnover across the PETM at
244 Allison Guyot were first described by Thomas [1998] and Thomas *et al.* [2000], but no
245 detailed information was provided, and the assemblage turnover across the ETM3 and
246 MECO has not been documented. Later, cylindrical taxa with complex apertures were
247 studied by Hayward *et al.* [2012]. Here we document for the first time the late
248 Paleocene to Eocene benthic foraminiferal assemblages from this Pacific seamount, and
249 look into faunal turnover across hyperthermal events.

250

251 3. Methods

252 A set of 97 samples were analyzed, covering the upper Paleocene (planktic
253 foraminiferal zones P3b-P5, calcareous nannofossil zones NP4-NP9) through lower-
254 middle Eocene (P5-P15, NP9-NP18; Figure S2). The sampling resolution varied
255 between 2 cm (in the intervals of expected hyperthermals) to 1.5 m (1 sample per core
256 section). Samples were oven-dried at 60°C, soaked in warm water with detergent, and
257 wet-sieved over a 63 µm sieve. Samples were weighed before and after sieving to
258 determine the weight percent of the coarse fraction (CF %) in order to evaluate
259 winnowing (thus probably current intensity) over time. Coarse fraction weight % is
260 considered as a proxy for winnowing, especially on top guyot settings, because
261 sediments deposited under these hydrographic conditions tend to experience winnowing
262 by bottom currents both during deposition and shortly thereafter [*Bralower and*
263 *Mutterlose, 1995*].

264 Quantitative analyses of benthic foraminiferal assemblages were based on 300
265 individuals per sample from the >63 µm size fraction (Table S1), and allowed us to
266 infer such parameters as paleodepth, bottom current velocity, oxygen concentration of
267 the bottom waters and the quantity and quality of organic matter reaching the seafloor
268 [*Jorissen et al., 2007*]. We followed the generic classification by *Loeblich and Tappan*
269 [1987] as modified by *Hayward et al. [2012]* for uniserial taxa with complex apertures,
270 and *Tjalsma and Lohmann [1983]*, *van Morkhoven et al. [1986]*, *Alegret and Thomas*
271 [2001] and *Hayward et al. [2012]* for determinations at the species level (Figure S3).
272 The relative abundance of selected species and morphological supra-generic groups
273 (Tables 2, S2, S3) were used to infer the paleoenvironmental turnover across the studied
274 events. Some of the supra-generic groups include cylindrical taxa with complex

275 apertures (with rectilinear, generally uniserial tests), buliminids and bolivinids *sensu*
276 *stricto* (*s.s.*) and buliminids *sensu lato* (*s.l.*).

277 The relative abundance of the infaunal buliminid group was calculated, as this
278 group of detrital feeders tolerates reduced oxygen concentrations [*Sen Gupta and*
279 *Machain-Castillo*, 1993] and/or thrives under an abundant food supply [*Thomas*, 1998;
280 *Fontanier et al.*, 2002; *Jorissen et al.*, 2007] in modern oceans. All species were
281 allocated into habitat-related morphogroups (infaunal vs. epifaunal; Table S4), which in
282 general can be used as proxies for oxygenation and trophic conditions at the seafloor,
283 with high relative abundance of infaunal taxa thought to be indicative of a high food
284 supply and/or low oxygen availability [e.g., *Jorissen et al.*, 1995; 2007]. However this
285 parameter must be used with caution, because even for many living taxa the relation
286 between morphology and microhabitat has not been well established [e.g., *Jorissen*,
287 1999], and assignments may be correct only about 75% of the times [*Buzas et al.*,
288 1993].

289 The Fisher- α diversity index and the Shannon-Weaver heterogeneity index were
290 calculated. The former correlates the number of species and the number of individuals
291 in each sample [*Murray*, 2006], and the latter depends on the relative abundance and the
292 number of taxa [*Hammer and Harper*, 2006]. The benthic foraminiferal accumulation
293 rate (BFAR), i.e. the number of benthic foraminifera per cm² per thousand years, is a
294 proxy for export productivity, with higher numbers indicating more organic carbon
295 reaching the seafloor [*Herguera and Berger*, 1991; *Jorissen et al.*, 2007]. BFARs were
296 calculated using data on dry bulk density [*Sager et al.*, 1993], and data on CF% and
297 number of foraminifera per gram. BFARs have been used extensively to estimate the
298 flux of food to the seafloor [*Herguera and Berger*, 1991; *Jorissen et al.*, 2007]. We can,
299 however, not assume that BFARs on seamounts reflect primary productivity in the

300 surface waters, in contrast with e.g. the region studied by *Herguera and Berger* [1991]
301 to define BFAR, because of the biophysical coupling of food supply to current regime
302 [e.g., *Genin*, 2004].

303 The age model is mainly based on the calcareous nannofossil stratigraphy
304 [*Bralower and Mutterlose*, 1995; *Bralower et al.*, 1995a, b]. We used the
305 biostratigraphic datum levels in *Bralower et al.* [1995a], recalculated ages to the modern
306 time scale as in *Yamaguchi and Norris* [2015], but our age scale differs from that in
307 these authors by placing the base of the PETM at 55.5 Ma. We then fine-tuned the
308 biostratigraphy through correlation of the stable isotope stratigraphy with that of *Littler*
309 *et al.* [2014]. We overlaid the low resolution record from Site 865 over the high
310 resolution record in *Littler et al.* [2014], then minimized the differences between the
311 low resolution curve and a 7 pt moving average of the *Littler et al.* [2014] curve.

312

313 **4. Results**

314 The weight % coarse fraction (CF%) ranges between 10 and 60% (Figure 2),
315 with higher values in the uppermost Paleocene-lowermost Eocene (between 47.8-59.9
316 Ma), and a marked drop at about 47.8 Ma, followed by a slight increase between 43 and
317 40 Ma, i.e. before the MECO. Low values in the lowermost 2 samples cannot be
318 evaluated due to poor preservation. The CF% is negatively correlated with benthic
319 foraminiferal $\delta^{18}\text{O}$ values (Figure 2), with highest CF% during the warmest periods
320 (Figures 3, 4).

321 In contrast to planktic foraminifera, which lived in surface waters, the benthic
322 foraminiferal specimens which secrete their tests in deep-waters and have much less
323 porous walls than planktics, are well preserved, the ornamentation of their tests (e.g.
324 spines) is clearly recognized, and they show no evidence for recrystallization. Benthic
325 foraminiferal assemblages at Site 865 are diverse and heterogeneous (Figure 2).

326 Agglutinated foraminifera and lenticulinids, a dissolution-resistant group, make up less
327 than 9% and 11% of the assemblages, respectively (Table S1; Figure S4). Assemblages
328 are dominated by infaunal morphogroups (mean values ~80%), including buliminids *s.l.*
329 and cylindrical taxa with complex apertures, generally dominated by species of the
330 genera *Strictocostella* and *Siphonodosaria* (Figure 2) that are included in the group
331 Stilostomellidae [Hayward *et al.*, 2012; Appendix 16]. Overall, BFAR values are low
332 across the studied interval, and the most prominent, positive peaks are recorded within
333 the PETM, coinciding with high percentages of buliminid taxa (Figure 5), and below the
334 MECO (Figure 2). Among epifaunal taxa, *Cibicidoides* spp. are common in the
335 lowermost Eocene, and *Nuttallides truempyi* in the upper Ypresian-lower Lutetian
336 (Figure 2). The assemblages gradually decrease in diversity and heterogeneity in the
337 uppermost Paleocene, and decline markedly at the Paleocene/Eocene boundary during
338 the Benthic Extinction Event (BEE). Diversity indices only show a very minor decrease
339 across the ETM3, and no significant variations in the interval where the MECO should
340 be located (Figure 2).

341 Paleocene assemblages are diverse and dominated by infaunal taxa such as
342 buliminids *s.s.*, bolivinids *s.s.* and cylindrical taxa (Figure 2), mainly stilostomellids,
343 with *Strictocostella pseudoscripta/spinata* as the most common species [Hayward *et al.*,
344 2012].

345 The turnover across the BEE is marked by the extinction of 10.4% of species
346 and the local/regional last occurrence of 22.9% of species (Table S5). Agglutinated taxa
347 are almost absent across the PETM (Figures 2, 3). Infaunal taxa, such as buliminids *s.s.*
348 (e.g., *Bulimina semicostata*, *B. simplex*) and bolivinids *s.s.* (e.g., *B. decoratus*,
349 *Tappanina selmensis*) sharply increased in relative abundance across the peak CIE. The
350 cylindrical taxa temporarily declined in abundance (Figure 3), especially the spinose

351 stilostomellids, but the percentage of smooth-walled pleurostomellids (Figure S4)
352 increased [Hayward *et al.*, 2012]. The whole group of cylindrical taxa with complex
353 apertures did not show significant net extinction during the PETM [Hayward *et al.*,
354 2012]. The epifaunal *N. truempyi* is very rare immediately above the extinction event,
355 and the few specimens present have a pre-extinction carbon isotope signature, thus were
356 bioturbated into the lower Eocene [Bralower *et al.*, 1995 a, b]. The shallow infaunal
357 buliminids show the clear signature of the PETM CIE [Zachos *et al.*, 2001]. Large, flat
358 *Cibicidoides* species peak in relative abundance above the CIE, but specimens with a
359 CIE stable isotope signature occur right below the base of the CIE, and thus are
360 probably bioturbated or brought to that level by coring disturbance.

361 Overall, BFARs increased across the PETM but show large fluctuations. The
362 CF% fluctuated during the first ~20 kyr of the event, and increased 60 kyr after the P/E
363 boundary coeval with the initial recovery of $\delta^{13}\text{C}$ values in benthic foraminifera, a
364 gradual decrease in the percentage of buliminids *s.l.* and an increase in relative
365 abundance of large discoidal *Cibicidoides* (Figure 5).

366 Lower Eocene assemblages (between ~55 and 52.5 Ma) contain slightly higher
367 percentages of dissolution-resistant forms such as lenticulinids and *Oridorsalis*
368 *umbonatus*, as well as common *Cibicidoides* species and opportunistic taxa such as
369 *Aragonia aragonensis* (Figures 3, S4). The percentage of *Cibicidoides* spp. gradually
370 decreased across this interval, and cylindrical taxa recovered their pre-PETM abundance
371 values.

372 Low sedimentation rates preclude identification of the ETM2, but a prominent
373 increase in relative and absolute abundance of *N. truempyi* at ~53.7 Ma coincided with,
374 or just post-dated this event. The identification of ETM3 at Site 865 is based on low
375 $\delta^{13}\text{C}$ values in *Cibicidoides* and *N. truempyi* (Figures 2, 6). No significant extinctions

376 have been recorded across this event (Table S5), but faunal changes include a slight
377 increase in the percentage of buliminids *s.l.* (Figure 2) and an abundance peak of *A.*
378 *aragonensis* (Figure 6).

379 The percentage of cylindrical taxa (stilostomellids and uniserial lagenids) and
380 agglutinated taxa increased ~170 kyr after the ETM3, coinciding with a sharp decrease
381 in *N. truempyi* and a slight decrease in % buliminids *s.l.* The relative abundance of
382 buliminids *s.l.*, *Cibicidoides* spp., *B. decoratus*, *Globocassidulina subglobosa*,
383 *Nuttallides umbonifera*, *Pyramidina rudita* and *Gyroidinoides* spp. increased ~238 kyr
384 after ETM3, coeval with a decrease in relative abundance of cylindrical taxa (Figure 6).

385 The relative abundance of *N. truempyi* decreased markedly in the upper half of
386 the studied interval (~51.5 – 36.5 Ma), coeval with an increasing trend in buliminids *s.l.*
387 and cylindrical taxa (Figures 2, S4), which are largely dominated by the species most
388 abundant throughout the studied interval, *Strictocostella pseudoscripta* [Hayward *et al.*,
389 2012]. A prominent decrease in CF% occurred at ~47 Ma.

390 The MECO event at ~ 40 Ma [Bohaty *et al.* 2009; Westerhold and Röhl, 2013]
391 was not recognized in the isotope record at the resolution of our studies. This age
392 interval coincides with very low BFAR values at Site 865, immediately above the
393 largest peak in BFAR. Benthic assemblages at ~40 Ma are characterized by a decrease
394 in abundance of stilostomellids and *N. truempyi*, and by a slight increase in buliminids
395 *s.l.*, pleurostomellids and uniserial lagenids (Figure S4, Table S1).

396

397 **5. Discussion**

398 **5.1. Coarse fraction weight %**

399 At Site 865, the CF% is above 10% in almost all samples, and above 25% in
400 many samples (Figure 2). This is unusually high as compared to carbonate oozes at

401 other drill sites, e.g. Walvis Ridge and Maud Rise [e.g., *Kelly et al.*, 2010, 2012]. This
402 high CF%, dominated by planktic foraminifera, probably reflects current winnowing on
403 the seamount, which removed the fine (calcareous nannoplankton) fraction [e.g., *Sager*
404 *et al.*, 1993]. Changes in CF% thus can be seen as reflecting current activity across the
405 top of Allison Guyot, with higher values indicating more winnowing. Increased
406 winnowing occurred during warmer periods, with peak CF% across the PETM, a
407 smaller peak across ETM3, and generally high values throughout the warm early
408 Eocene, followed by a decline coeval with the high latitude cooling starting in the early
409 middle Eocene (Figures 2, 4).

410 Such increased current activity during warm periods might appear surprising,
411 because warm time periods have traditionally been seen as characterized by ‘sluggish
412 ocean circulation’ [e.g. *Fischer and Arthur*, 1977; see review in *Thomas et al.*, 2000].
413 Planktic foraminifera, which show a shift to deeper depth-habits by morozovellids and
414 acaraninids, indicate that the water column structure changed during PETM warming
415 [*Kelly et al.*, 1996, 1998], supported by climate modeling [*Winguth et al.*, 2012]. Such
416 changes in stratification may have influenced current patterns around the seamount
417 [*Lavelle and Mohn*, 2010]. In addition, in Greenhouse climates such as that of the early
418 Eocene sea surface temperatures are high, and intense hurricane activity drives a strong
419 mixing in the upper tropical oceans [*Korty et al.*, 2008]. Such increased hurricane
420 activity during warm climates [e.g., *Emanuel*, 2002; *Sriver and Huber*, 2007]] might
421 have supplied temporary increased energy for enhanced current activity over seamounts,
422 with deeper vertical mixing.

423 Alternatively, changes in deep water circulation [e.g. *Thomas*, 2004; *Thomas et*
424 *al.*, 2008; *Hague et al.*, 2012] may have contributed to increased current activity at Site
425 865. For example, the mixing of deep waters sourced from the Southern Ocean and the

426 North Pacific in the tropical Pacific during the Paleogene (~65 to ~45 Ma) [*Thomas et*
427 *al.*, 2008], together with the steep topography of the mid Pacific mountain chain may
428 have influenced the hydrodynamics around the seamount.

429 The use of CF (%), as a proxy for winnowing, points to a decrease in current
430 activity during the early Lutetian (Figures 2, 4). There is no evidence that surface waters
431 in the tropical region of Site 865 cooled at that time [*Pearson et al.*, 2007], and
432 stratification may have become more pronounced due to high latitude (thus deep water)
433 cooling, making deep mixing due to hurricane activity less pronounced. Alternatively,
434 current patterns may have been changed as the site was drifting northwards from ~2°N
435 (in the Paleocene) to 6°N (in the late Eocene) [*Bralower et al.*, 1995a], and the
436 geographic extent of the zone of highest hurricane activity may have changed [*Kossin et*
437 *al.*, 2014].

438

439 **5.2. Benthic foraminifera**

440 Benthic foraminiferal assemblages at Site 865 are highly diverse and
441 heterogeneous, as expected for deep-sea faunas. The strong dominance by calcareous
442 taxa throughout the studied interval is compatible with the location of this site at a
443 paleodepth of 1300-1500 m, considerably above the CCD during most of the studied
444 time interval [*Pälike et al.*, 2012]. The benthic foraminifera on Allison Guyot Site 865
445 generally represent cosmopolitan taxa [*Thomas*, 1998; *Hayward et al.*, 2012], and no
446 endemic species were identified, supporting the observations on modern taxa of the
447 importance of a motile life stage [*Alve and Goldstein*, 2003; 2010].

448 The dominance of long-term assemblages by infaunal taxa (mainly cylindrical
449 taxa) throughout the studied interval, in an oligotrophic setting as inferred from planktic
450 foraminifera [*Kelly et al.*, 1996, 1998] and calcareous nannofossils [*Bralower et al.*,

451 1995a], and at low overall BFAR values appears unexpected, but we argue that this
452 might reflect a seamount-top ecosystem. Interpretation of species abundances is
453 complex in seamount settings, where the selective advantage of morphotypes under an
454 active current regime must be considered. Attached epifaunal taxa are abundant under
455 such conditions [e.g., *Schoenfeld*, 2002], and detritivore infaunal taxa are generally rare
456 because the sediment contains insufficient fine-grained organic matter to support
457 deposit feeders [*Heinz et al.*, 2004]. However, both infaunally positioned suspension
458 feeders anchored by spines, and attached epifaunal suspension feeders may be common.
459 We suggest that the spinose cylindrical taxa most common throughout the studied
460 interval (Stilostomellid species of the genus *Strictocostella*) [*Hayward et al.*, 2012] may
461 have been shallow-infaunally living species, according to their shape, distribution and
462 carbon isotope signature [*Hayward and Kawagata*, 2005; *Hayward et al.*, 2012; *Mancin*
463 *et al.*, 2013], anchored in the sediment by their spines [*Hottinger*, 2000], and
464 suspension-feeding in the water column using their pseudopods extended through the
465 complex aperture [e.g. *Hottinger*, 2000; 2006; *Mancin et al.*, 2013]. Such a lifestyle
466 would be in agreement with suggestions that they were infaunal, k-strategist taxa with
467 low metabolic rates [*Mancin et al.*, 2013], and rules out the possibility of reworking as
468 the cause of their high numbers in the sediment. Consequently, we suggest that changes
469 in the assemblages over time dominantly reflect changes in current activity (thus food
470 brought to the benthic foraminifera) rather than changes in primary productivity, since
471 planktic foraminifera and nannofossils suggest decreased productivity during the PETM
472 [*Kelly et al.*, 1996; 1998]. Benthic foraminiferal assemblages do not show convincing
473 evidence for a strong decline in oxygen availability.

474 Unfortunately, we cannot simply interpret the CF% data in terms of relative
475 abundance of the spinose stilostomellids. Assemblages are easy to interpret only when

476 one specific environmental factor dominates, e.g. food supply, but interaction between
477 active currents and food transport (and, at times, changes in carbonate corrosivity)
478 means that critical thresholds may play a role [Murray, 2001]. Higher current activity
479 could result in lower food supply through more winnowing and removal of food
480 particles, or in increased food particles through trophic focusing.

481 In the late Paleocene, for instance, CF% increased slightly, while BFARs
482 declined gradually as did the relative abundance of stilostomellids, while the
483 oligotrophic indicator *N. truempyi* increased. The benthic foraminiferal data thus
484 indicate decreasing food supply to the benthos in the latest part of the Paleocene, while
485 current strength increased (Figure 7). During the earliest Eocene, however, and
486 especially during the PETM the correlations were more complex (see below), and
487 overall reversed, with higher cylindrical taxa% during high CF%. With the decline in
488 CF% at about 47 Ma, however, we again see negative correlation with cylindrical taxa%
489 (Figure 4). We argue that the situation during the PETM may reflect combined effects
490 of increasing current strength and ocean acidification.

491 The beginning of the PETM coincides with negative excursions in benthic
492 foraminiferal $\delta^{13}\text{C}$ and $\delta^{18}\text{O}$, and CaCO_3 dissolution, followed by reprecipitation, as
493 reflected in the occurrence of euhedral calcite crystals around foraminifera in the PETM
494 interval, and in that interval only (Figure S1) [Kozdon *et al.*, 2013]. The high % CaCO_3
495 content despite dissolution is probably related to the lack of fine-grained terrestrial
496 material in biogenic sediments deposited on the current-swept top of the guyot, so that
497 CaCO_3 dissolution could not result in formation of a clay layer. During carbonate
498 dissolution, pore waters may become highly saturated in carbonate [Ilyina and Zeebe,
499 2012], so that infaunal benthic foraminifera are shielded from the corrosive waters

500 [Foster et al., 2013], whereas epifaunal taxa are exposed and may no longer be able to
501 survive. High %CF values point to increased current activity (Figure 4).

502 At Site 865, as globally, large and heavily calcified taxa (e.g., *S. beccariiiformis*)
503 became extinct at the start of the PETM, and 33.4% (including local disappearances) of
504 the species suffered extinction. During the main phase of the CIE, the epifaunal *N.*
505 *truempyi*, living exposed to bottom waters, was ecologically displaced, as at Antarctic
506 Sites 689 and 690 [Thomas and Shackleton, 1996; Thomas, 2003]. We speculate that the
507 smooth-walled taxa (buliminids and pleurostomellids) may have lived deeper in the
508 sediment than the spinose suspension feeders, calcifying in less carbonate-
509 undersaturated pore waters, as did trochospiral infaunal species *Oridorsalis umbonatus*
510 at Walvis Ridge sites [Foster et al., 2013]. In the Wagner Basin (Gulf of California,
511 Mexico), buliminids are abundant without signs of dissolution under corrosive
512 conditions close to carbon dioxide-emitting vents [Hart et al., 2012]. These deeper
513 infaunal taxa thus could have become dominant (up to 96% of the assemblages) even at
514 high current activity (maximum CF%, Figures 2, 3) and in the absence of a higher food
515 supply, through lack of competition of epifaunal and shallow infaunal species which
516 could not survive in the CaCO₃-corrosive waters. Possibly, however, more food may
517 have become available to infaunal deposit feeders even at declining primary
518 productivity [Kelly et al., 1996; Winguth et al., 2012], because changing current
519 conditions might have led to trophic focusing at the location of Site 865, thus enhanced
520 BFAR values and higher percentages of buliminids and pleurostomellids. The scarcity
521 of ostracodes, organisms without a motile life stage [Yamaguchi and Norris, 2015]
522 might have been caused not by a decline in food, but by carbonate corrosiveness and the
523 high current regime, followed by lack of re-immigration.

524 High relative abundances of small, thin-walled abyssamminid species directly
525 after the benthic extinction have been documented at many sites [Thomas, 1998], e.g. on
526 Pacific Shatsky Rise Sites 1209-1211 [Takeda and Kaiho, 2007], on Southeast Atlantic
527 Walvis Ridge Sites 525 and 527 [Thomas and Shackleton, 1996], and the western
528 Tethys [Alegret et al., 2009a], but these species are absent during the PETM at Site 865
529 (Figure 3). We suggest that these small species may have not been able to thrive under
530 the current conditions on the seamount, or the food supply may have been too high for
531 these abyssal species adapted to very oligotrophic conditions.

532 At about 80 kyr after the beginning of the PETM, large and flat *Cibicidoides*
533 with coarse pores on the spiral side increased in relative abundance, an unusual feature
534 for PETM assemblages [Thomas, 1998]. Possibly, these species resembled the living
535 *Cibicidoides wuellerstorfi* [Lutze and Thiel, 1989] or *Cibicidoides lobatulus* [Dubicka et
536 al., 2015; Gooday et al., 2015], living epifaunally attached to hard surfaces [Thomas,
537 1998]. These epifaunal species could not thrive during the phase of deep-sea ocean
538 acidification during peak PETM, but they may have become abundant when currents
539 were still too strong to allow re-establishment of the shallow infaunal suspension
540 feeders [Schoenfeld, 2002] and corrosiveness declined. We do not know whether the
541 *Cibicidoides* were current-distributed from outcropping rock surface towards the edge
542 of the guyot, or lived attached to sessile animals close to the location of Site 865.
543 Subsequently, the percentage of *Cibicidoides* spp. gradually decreased, probably due to
544 less transport of shells or to decreased food supply associated with declining current
545 strength. After the dissolution interval of the PETM, CF% (thus possibly current
546 strength) declined, the abundance of buliminids *s.l.* (including the opportunistic species
547 *T. selmensis*) decreased and the abundance of the cylindrical and spinose stilostomellids
548 (including *S. pseudoscripta*) increased again.

549 No evidence for significant dissolution (euhedral calcite crystals) has been
550 observed across the ETM3 at Site 865. A moderate increase in food supply to the
551 seafloor is inferred from increased BFAR values and percentage of buliminids *s.l.*
552 (Figures 2, 7). The species *P. rudita* shows greatest abundances at intermediate
553 paleodepths [Tjalsma and Lohmann, 1983], hence its increase in abundance after the
554 ETM3 may be related to an increased food availability, which allowed this species to
555 thrive at somewhat greater paleodepths, such as at Site 865. The species *A. aragonensis*
556 is a potentially opportunistic species [Steineck and Thomas, 1996], which has been
557 interpreted as a marker of hyperthermal events due to its proliferation during and after
558 Paleogene warming events [Thomas, 1990, 1998, 2003; Alegret *et al.*, 2009a, b;
559 Giusberti *et al.*, 2009; Ortiz *et al.*, 2011]. The species peaked in abundance after the
560 PETM [Thomas, 1998] and during the ETM3 at Site 865, supporting the interpretation
561 of this species as a marker of early Eocene hyperthermal events. This species may have
562 proliferated during warm intervals but not under carbonate-corrosive conditions, which
563 would explain why its abundance peak occurred after the peak PETM.

564 In the upper half of the studied interval (~51.5 – 36.5 Ma; after ETM3, then
565 following the unconformity), a moderate increase in the food supply to the benthos is
566 inferred from the gradual decrease in relative abundance of *N. truempyi* and higher
567 percentages of buliminids *s.s.* and cylindrical taxa (Figure 2), with lower CF% once
568 again associated with other benthic indicators of somewhat higher food supply, as in the
569 late Paleocene. A slight increase is recorded from 43 to 40 Ma, possibly related to more
570 intense winnowing by currents towards the MECO.

571 We thus interpret the late Paleocene – middle Eocene benthic assemblages on a
572 Pacific seamount during a warming-cooling long-term evolution punctuated by short
573 hyperthermal events as follows:

574 1) The dominance of infaunal, cylindrical taxa with complex apertures reflects
575 the ecological success of these shallowly infaunal dwelling suspension feeders in the
576 current-swept environment of the guyot-top. This group was, however, less successful
577 under the CaCO₃ corrosive conditions of the PETM, and declined in abundance (Figure
578 5), with spinose stilostomellids being replaced by smooth-walled pleurostomellids
579 (Figure S4).

580 2) Buliminids *s.l.* increased in relative abundance in intervals with increased
581 %CF and decreased percentages of *N. truempyi*, an oligotrophic species (Figure 5).
582 Their increased relative abundance may have been due to increased food supply because
583 of trophic focusing during the PETM or around the MECO interval, independent of
584 primary productivity. Alternatively, this group may have proliferated under CaCO₃
585 corrosive conditions, as their deeper infaunal life style in less under-saturated pore
586 waters may have protected them (e.g. during the PETM) [Foster *et al.*, 2013].

587 3) The infaunal cylindrical taxa may have lived closer to the sediment-water
588 interface because of their suspension-feeding lifestyle than the deposit-feeding
589 buliminids, thus were less sheltered from dissolution. Lenticulinids, another dissolution-
590 resistant group with an infaunal life style, did not peak in abundance at Site 865,
591 probably as a consequence of their different feeding strategy and lack of ecological
592 success where suspension feeders thrive.

593 4) The highest % of coarse fraction occurred during the recovery period of the
594 PETM and overlaps with high relative abundances of *Cibicidoides* spp. (Figure 5),
595 reflecting the adaptation of these species to high current conditions attached to hard
596 surfaces [Thomas, 1998], but they live epifaunally and have coarse pores, thus are
597 susceptible to dissolution and cannot thrive under CaCO₃ corrosive conditions.

598 5) The distribution pattern of *N. truempyi*, which in the upper Paleocene is
599 negatively correlated to BFAR and positively to CF%, is interpreted as indicative of
600 oligotrophic conditions. The high abundances of this species during the early-mid
601 Eocene (53.7 to ~44 Ma) were also correlated to intervals with higher CF% and lower
602 cylindrical taxa %, thus more oligotrophic conditions. Its disappearance during the
603 PETM may reflect the occurrence of combined CaCO₃ corrosive waters, a high current
604 regime, and/or ecological competition with taxa benefited from increased food
605 availability. The species is generally common during warm conditions [e.g. *Takeda and*
606 *Kaiho*, 2007; *Alegret et al.*, 2009a, b; *Giusberti et al.*, 2009; *Boscolo-Galazzo et al.*,
607 2013], and at Site 865 its abundance declined towards the upper part of the middle
608 Eocene, coinciding with progressive cooling of sea-bottom waters as inferred from
609 higher benthic $\delta^{18}\text{O}$ values (Figure 2).

610 In spite of the unusual conditions on a seamount setting, the extinction of
611 benthic foraminifera at the start of the PETM is comparable to that at other sites where
612 more than 30% of the species went extinct or temporarily disappeared [e.g., *Thomas*,
613 1990; *Thomas and Shackleton*, 1996; *Takeda and Kaiho*, 2007; *Alegret et al.*, 2009a, b].
614 The geographic isolation of the seamount thus does not seem to have affected the
615 extinction and recovery of the assemblages after the PETM, in contrast with ostracodes,
616 which show more severe extinction and a much longer recovery period at Allison Guyot
617 [*Yamaguchi and Norris*, 2015] than in the North Atlantic [*Yamaguchi and Norris*, 2012]
618 and the Southern Ocean [*Steineck and Thomas*, 1996; *Webb et al.*, 2009]. This
619 differential response in ostracodes to the PETM probably results from the fact that
620 benthic ostracodes are not efficient in dispersal [*Yasuhara et al.*, 2012; *Yamaguchi and*
621 *Norris*, 2015], whereas benthic foraminifera are highly efficient [*Alve and Goldstein*,
622 2003, 2010].

623

624 **6. Conclusions**

625 Pelagic sediments deposited on the flat top of Allison Guyot (Mid-Pacific
626 Mountains) at equatorial Pacific ODP Site 865 provide an long term record of benthic
627 foraminifera across the late Paleocene – middle Eocene, and allow us to reconstruct the
628 faunal and paleoenvironmental turnover in an unusual, isolated and current-swept
629 seamount setting. The late Paleocene was characterized by a progressive increase in
630 current activity and oligotrophic conditions, but the food input at the Paleocene-Eocene
631 boundary suddenly appeared to increase even under declining primary productivity.
632 These conditions of high current activity and food supply persisted until ~54 Ma.
633 Afterwards, the food supply was moderate and oligotrophic taxa like *N. truempyi* started
634 to dominate the assemblages up to the middle Eocene (~43 Ma). Current activity
635 gradually increased (~42 Ma) after a drop at the middle Eocene (~47 Ma), and remained
636 relatively high up to the Priabonian, although it did not reach the high activity recorded
637 during the late Paleocene-early Eocene.

638 Assemblage changes across the PETM and ETM3 were similar, with both events
639 possibly associated with increased food supply through trophic focusing. Faunas across
640 the PETM may have been affected by a combination of carbonate corrosion and locally
641 increased food supply through trophic focusing due to enhanced current activity,
642 followed by increased current activity after recovery from carbonate dissolution,
643 whereas trophic focusing was not associated with severe dissolution during ETM3.

644 The benthic foraminiferal turnover at Allison Guyot was controlled by a
645 combination of long-term global change and superimposed short-term hyperthermal
646 events, through changes in local current systems around the guyot-top rather than
647 changes primary productivity or organic remineralization.

648

649 **Acknowledgments**

650 This research used samples provided by the Ocean Drilling Program (ODP), sponsored
651 by the U.S. National Science Foundation (NSF) and participating countries under
652 management of Joint Oceanographic Institutions (JOI), Inc. G.J.A.R. and L.A.
653 acknowledge funding from project CGL2014-58794-P (Spanish Ministry of Economy
654 and Competitiveness), and E.T. from NSF OCE-720049 and the Leverhulme Trust.
655 G.J.A.R. thanks the Consejo Nacional de Ciencia y Tecnología (Conacyt, México) for
656 her predoctoral fellowship. We acknowledge the comments of three anonymous
657 reviewers. All the data employed in this paper are available in the supplementary
658 information (Tables S1-S5), and may also be requested to Gabriela Arreguín-Rodríguez
659 (arreguin@unizar.es) or Laia Alegret (laia@unizar.es).

660

661 **References**

662 Agnini, C., P. Macrì, J. Backman, H. Brinkhuis, E. Fornaciari, L. Giusberti, V. Luciani,
663 D. Rio, A. Sluijs, and F. Speranza (2009), An early Eocene carbon cycle
664 perturbation at ~52.5 Ma in the Southern Alps: Chronology and biotic response,
665 *Paleoceanography*, 24, PA2209, doi:10.1029/2008PA001649.

666 Alegret, L., and E. Thomas (2001), Upper Cretaceous and lower Paleogene benthic
667 foraminifera from northeastern Mexico, *Micropaleontology*, 47(4), 269-316.

668 Alegret, L., and E. Thomas (2005), Cretaceous/Paleogene boundary bathyal paleo-
669 environments in the central North Pacific (DSDP Site 465), the Northwestern
670 Atlantic (ODP Site 1049), the Gulf of Mexico and the Tethys: The benthic
671 foraminiferal record, *Palaeogeography, Palaeoclimatology, Palaeoecology*, 224,
672 53-82, doi:10.1016/j.palaeo.2005.03.031.

673 Alegret, L., and E. Thomas (2009), Food supply to the seafloor in the Pacific Ocean
674 after the Cretaceous Paleogene boundary event, *Marine Micropaleontology*, 73,
675 105-116, doi:10.1016/j.marmicro.2009.07.005.

676 Alegret, L., S. Ortiz, and E. Molina (2009a), Extinction and recovery of benthic
677 foraminifera across the Paleocene-Eocene Thermal Maximum at the Alamedilla
678 section (Southern Spain), *Palaeogeography, Palaeoclimatology, Palaeoecology*,
679 279, 186-200.

680 Alegret, L., S. Ortiz, X. Orue-Etxebarria, G. Bernaola, J. I. Baceta, S. Monechi, E.
681 Apellaniz, and V. Pujalte (2009b), The Paleocene-Eocene Thermal Maximum:
682 new data on microfossil turnover at the Zumaia section, Spain, *Palaios*, 24, 318-
683 328.

684 Alegret, L., S. Ortiz, I. Arenillas, and E. Molina (2010), What happens when the ocean
685 is overheated? The foraminiferal response across the Paleocene–Eocene Thermal
686 Maximum at the Alamedilla section (Spain), *GSA Bulletin*, 122(9/10), 1616-
687 1624.

688 Alve, E., and S. T. Goldstein (2003), Propagule transport as a key method of dispersal
689 in benthic foraminifera (Protista), *Limnology and Oceanography*, 48, 2163–
690 2170.

691 Alve, E., and S. T. Goldstein (2010), Dispersal, survival and delayed growth of benthic
692 foraminiferal propagules, *Journal of Sea Research*, 63, 36–51.

693 Bohaty, S. M., and J. C. Zachos (2003), Significant Southern Ocean warming event in
694 the late middle Eocene, *Geology*, 31(11), 1017-1020.

695 Bohaty, S. M., J. C. Zachos, F. Florindo, and M. L. Delaney (2009), Coupled
696 greenhouse warming and deep-sea acidification in the middle Eocene,
697 *Paleoceanography*, 24, PA2207, doi:10.1029/2008PA001676.

698 Boomer, I., and R. Whatley (1995), Cenozoic Ostracoda from guyots in the western
699 Pacific: Holes 865B and 866B (Leg 143), in Proceedings of the Ocean Drilling
700 Program, Scientific results, vol. 143, edited by E. L. Winterer et al. pp. 75–86,
701 College Station, Texas, Ocean Drilling Program.

702 Boscolo-Galazzo, F., L. Giusberti, V. Luciani, and E. Thomas (2013),
703 Paleoenvironmental changes during the Middle Eocene Climatic Optimum
704 (MECO) and its aftermath: The benthic foraminiferal record from the Alano
705 section (NE Italy), *Palaeogeography, Palaeoclimatology, Palaeoecology*, 378,
706 22-35.

707 Boscolo-Galazzo, F., E. Thomas, M. Pagani, C. Warren, V. Luciani, and L. Giusberti
708 (2014), The Middle Eocene Climatic Optimum (MECO): a multi-proxy record
709 of paleoceanographic changes in the South-east Atlantic (ODP Site 1263, Walvis
710 Ridge), *Paleoceanography*, 29, 1143-1161, doi:10.1002/2014PA002670.

711 Boyd, P. W., and T. W. Trull (2007), Understanding the export of biogenic particles in
712 oceanic waters: Is there consensus?, *Progress in Oceanography*, 72, 276-312.

713 Bralower, T. J., and J. Mutterlose (1995), Calcareous nannofossil biostratigraphy of Site
714 865, Allison Guyot, central Pacific Ocean: a tropical Paleogene reference
715 section, in Proceedings of the Ocean Drilling Program, Scientific Results, vol.
716 143, edited by E. L. Winterer et al., pp. 31-74, College Station, Texas, Ocean
717 Drilling Program.

718 Bralower, T. J., J. C. Zachos, E. Thomas, M. Parrow, C. K. Paull, D. C. Kelly, I.
719 Premoli Silva, W. V. Sliter, and K. C. Lohmann (1995a), Late Paleocene to
720 Eocene paleoceanography of the equatorial Pacific Ocean: stable isotopes
721 recorded at Ocean Drilling Program Site 865, Allison Guyot, *Paleoceanography*,
722 10(4), 841-865, doi:10.1029/95PA01143.

723 Bralower, T. J., M. Parrow, E. Thomas, and J. C. Zachos (1995b), Data report: Stable
724 isotope stratigraphy of the Paleogene pelagic cap at Site 865, Allison Guyot, in
725 Proceedings of the Ocean Drilling Program, Scientific Results, vol. 143, edited
726 by E. L. Winterer et al., pp. 581-586, College Station, Texas, Ocean Drilling
727 Program.

728 Bukry, D. (1973), Low-latitude coccolith biostratigraphic zonation, in Initial Reports of
729 Deep Sea Drilling Project, vol. 15, edited by N. T. Edgar, J.B. Saunders et al.,
730 pp. 685-703, Washington, U. S. Government Printing Office.

731 Bukry, D. (1975), Coccolith and silicoflagellate stratigraphy, northwestern Pacific
732 Ocean, Deep Sea Drilling Project Leg 32, in Initial Reports of Deep Sea Drilling
733 Project, vol. 32, edited by R. L. Larson and R. Moberly et al., pp. 677-701,
734 Washington, U. S. Government Printing Office.

735 Burkett, A. M., A. E. Rathburn, M. E. Perez, L. A. Levin, H. Cha, and G. W. Rouse
736 (2015), Phylogenetic placement of *Cibicidoides wuellerstorfi* (Scwager, 1866)
737 from methane seeps and non-seep habitats on the Pacific margin, *Geobiology*,
738 13, 44-52.

739 Buzas, M. A., S. J. Culver, and F. J. Jorissen (1993), A statistical evaluation of the
740 microhabitats of living (stained) infaunal benthic foraminifera, *Marine*
741 *Micropaleontology*, 20, 311-320.

742 Chun, C. O. J., M. L. Delaney, and J. C. Zachos (2010), Paleoredox changes across the
743 Paleocene-Eocene thermal maximum, Walvis Ridge (ODP Sites 1262, 1263, and
744 1266): Evidence from Mn and U enrichment factors, *Paleoceanography*, 25,
745 PA4202, doi:10.1029/2009PA001861.

746 Colosimo, A. B., T. J. Bralower, and J. C. Zachos (2005), Evidence for lysocline
747 shoaling and methane hydrate dissociation at the Paleocene- Eocene thermal

748 maximum on Shatsky Rise, in Proceedings of the Ocean Drilling Program,
749 Scientific Results, vol. 198, edited by T. J. Bralower, I. Premoli Silva, and M. J.
750 Malone, 36 pp., Texas A&M Univ., College Station, Tex.

751 Cramer, B. S., J. D. Wright, D. V. Kent, and M. Aubry (2003), Orbital climate forcing
752 of the $\delta^{13}\text{C}$ excursions in the late Paleocene-early Eocene (chrons C24n-C25n),
753 *Paleoceanography*, 18(4), 1097, doi:10.1029/2003PA000909.

754 de Conto, R. M., S. Galeotti, M. Pagani, D. Tracy, K. Schaefer, T. Zhang, D. Pollard,
755 and D. J. Beerling (2012), Past extreme warming events linked to massive
756 carbon release from thawing permafrost, *Nature*, 484, 87-91.

757 de Forges, B. R., J. A. Koslow, and G. C. B. Poore (2000), Diversity and endemism of
758 the benthic seamount fauna in the southwest Pacific, *Nature*, 405, 944-947.

759 d'Haenens, S., A. Bornemann, P. Stassen, and R. Speijer (2012), Multiple early Eocene
760 benthic foraminiferal assemblages and $\delta^{13}\text{C}$ fluctuations at DSDP Site 401 (Bay
761 of Biscay – NE Atlantic), *Marine Micropaleontology*, 88-89, 15-35.

762 Dickens, G. R. (2011), Down the rabbit hole: toward appropriate discussion of methane
763 release from gas hydrate systems during the Paleocene–Eocene Thermal
764 Maximum and other past hyperthermal events, *Climate of the Past*, 7(3), 831–
765 846.

766 Dickens, G. R., J. R. O'Neil, D. K. Rea, and R. M. Owen (1995), Dissociation of
767 oceanic methane hydrate as a cause of the carbon isotope excursion at the end of
768 the Paleocene, *Paleoceanography*, 10(6), 965-971, doi:10.1029/95PA02087.

769 Dickens, G. R., M. M. Castillo, and J. C. G. Walker (1997), A blast of gas in the latest
770 Paleocene: Simulating first-order effects of massive dissociation of oceanic
771 methane hydrate, *Geology*, 25(3), 259-262.

772 Dower, J. F., and R. D. Brodeur (2004), The role of biophysical coupling in
773 concentrating marine organisms around shallow topographies, *Journal of Marine*
774 *Science*, 50, 1-2.

775 Dubicka, Z., M. Zlotnik, and T. Borszcz (2015), Test morphology as a function of
776 behavioral strategies – Inferences from benthic foraminifera, *Marine*
777 *Micropaleontology*, 116, 38-49.

778 Dunkley Jones, T., D. J. Lunt, D. N. Schmidt, A. Ridgwell, A. Sluijs, P. J. Valdes, and
779 M. A. Maslin (2013), Climate model and proxy data constraints on ocean
780 warming across the Paleocene-Eocene Thermal Maximum, *Earth Science*
781 *Reviews*, 125, 123-145.

782 Edgar, K. M., P. A. Wilson, P. F. Sexton, and Y. Suganuma (2007), No extreme bipolar
783 glaciation during the main Eocene calcite compensation shift, *Nature*, 448, 908-
784 911.

785 Edgar, K., E. Anagnostou, P. N. Pearson, and G. L. Foster (2015), Assessing the impact
786 of diagenesis on $\delta^{11}\text{B}$, $\delta^{13}\text{C}$, $\delta^{18}\text{O}$, Sr/Ca and B/Ca values in fossil planktic
787 foraminiferal carbonate, *Geochimica et Cosmochimica Acta*, 166, 189-209.

788 Eldrett, J. S., D. R. Greenwood, M. Polling, H. Brinkhuis, and A. Sluijs (2014), A
789 seasonality trigger for carbon injection at the Paleocene Eocene Thermal
790 Maximum, *Climate of the Past*, 10, 759-769.

791 Emanuel, K. (2002), A simple model of multiple climate regimes, *Journal of*
792 *Geophysical Research (Atmospheres)*, 107, 4077.

793 Fischer, A. G., and M. A. Arthur (1977), Secular variations in the pelagic realm, *SEPM*
794 *Special Publication*, 25, 19-50.

795 Fontanier, C., F. J. Jorissen, L. Licari, A. Alexandre, P. Anschutz, and P. Carbonel
796 (2002), Live benthic foraminiferal faunas from the Bay of Biscay: faunal
797 density, composition, and microhabitats, *Deep Sea Research I*, 49, 751-785.

798 Foster, L. C., D. N. Schmidt, E. Thomas, S. Arndt, A. Ridgwell (2013), Surviving rapid
799 climate change in the deep sea during the Paleogene hyperthermals, *PNAS*, 1-4.

800 Galeotti, S., S. Krishnan, M. Pagani, L. Lanci, A. Gaudio, J. C. Zachos, S. Monechi, G.
801 Morelli, and L. Lourens (2010), Orbital chronology of Early Eocene
802 hyperthermals from the Contessa Road section, central Italy, *Earth and Planetary
803 Science Letters*, 290, 192-200.

804 García-Muñoz, M., N. López-González, J. L. Rueda, D. Palomino, J. T. Vázquez, V.
805 Díaz-del-Río, and M. C. Fernández-Puga (2012), Caracterización ambiental de
806 montes submarinos del Mar de Alborán a partir del estudio de los sedimentos y
807 las asociaciones de foraminíferos bentónicos, *Geogaceta*, 52, 165-168.

808 Genin, A., P. K. Dayton, P. F. Lonsdale, and F. N. Spiess (1998), Corals on seamount
809 peaks provide evidence of current acceleration over deep-sea topography,
810 *Nature*, 322, 59-61.

811 Genin, A. (2004), Bio-physical coupling in the formation of zooplankton and fish
812 aggregations over abrupt topographies, *Journal of Marine Systems*, 50, 3-20.

813 Giusberti, L., R. Coccioni, M. Sprovieri, and F. Tateo (2009), Perturbation at the sea
814 floor during the Paleocene-Eocene Thermal Maximum: Evidence from benthic
815 foraminifera at Contessa Road, Italy, *Marine Micropaleontology*, 70, 102-119.

816 Gooday, A. J., A. Goineua, and I. Voltski (2015), Abyssal foraminifera attached to
817 polymetallic nodules from the eastern Clarion Clipperton Fracture Zone: a
818 preliminary description and comparison with North Atlantic dropstone
819 assemblages, *Marine Biodiversity*, doi 10.1007/s12526-014-0301-9.

820 Handley, L., P. N. Pearson, I. K. McMillan, and R. D. Pancost (2008), Large terrestrial
821 and marine carbon and hydrogen isotope excursions in a new Paleocene/Eocene
822 boundary section from Tanzania, *Earth Planetary Science Letters*, 275, 17–25.

823 Hart, M., L. Pettit, D. Wall-Palmer, C. Smart, J. Hall-Spencer, A. Medina-Sanchez, R.
824 M. Prol Ledesma, R. Rodolfo-Metalpa, and P. Collins (2012), Investigation of
825 the calcification response of foraminifera and pteropods to high CO₂
826 environments in the Pleistocene, Paleogene and Cretaceous, paper presented at
827 European Geosciences Union General Assembly 2012, Vienna, Austria.

828 Hay, W., R. M. de Conto, C. N. Wold, K. M. Wilson, S. Voigt, M. Schulz, A. R. Wold,
829 W. C. Dullo, A. B. Ronov, A. N. Balukhovsky, and E. Söding (1999),
830 Alternative global Cretaceous paleogeography, in *Evolution of the Cretaceous*
831 *ocean-climate system*, vol. 332, edited by E. Barrera, and C. C. Johnson, pp. 1–
832 47, Geological Society of America Special Paper.

833 Hayward, B. W., and S. Kawagata (2005), Extinct Foraminifera figured in Brady's
834 Challenger Report, *Journal of Micropalaeontology*, 26, 171-175.

835 Hayward, B., K. Johnson, A. T. Sabaa, S. Kawagata, and E. Thomas (2010), Cenozoic
836 record of elongate, cylindrical deep-sea benthic Foraminifera in the North
837 Atlantic and equatorial Pacific Oceans, *Marine Micropaleontology*, 74, 75-95.

838 Hayward, B. W., S. Kawata, A. Sabaa, H. Grenfell, L. van Kerckhoven, K. Johnson, and
839 E. Thomas (2012), The last global extinction (Mid-Pleistocene) of deep-sea
840 benthic foraminifera (Chrysalogoniidae, Ellipsoidinidae, Glandulonodosariidae,
841 Plectofrondiculariidae, Pleurostomellidae, Stilostomellidae), their Late
842 Cretaceous-Cenozoic history and taxonomy, Cushman Foundation for
843 Foraminiferal Research Special Publications, 43.

844 Heinz, P., D. Ruepp, and C. Hemleben (2004), Benthic foraminifera assemblages at
845 Great Meteor Seamount, *Marine Biology*, 144, 985-998.

846 Henson, S., R. Sanders, and E. Masden (2012), Global patterns in efficiency of
847 particulate organic carbon export and transfer to the deep ocean, *Global*
848 *Biogeochemical Cycles*, 26, GB1028, doi:10.1029/2011GB004099.

849 Herguera, J. C., and W. H. Berger (1991), Paleoproductivity from benthic foraminifera
850 abundance: Glacial to postglacial change in the west-equatorial Pacific,
851 *Geology*, 19, 1173-1176.

852 Higgins, J. A., and D. P. Schrag (2006), Beyond methane: Towards a theory for the
853 Paleocene- Eocene thermal maximum, *Earth and Planetary Science Letters*, 245,
854 523-537.

855 Hottinger, L. C. (2000), Functional morphology of benthic foraminiferal shells,
856 envelopes of cells beyond measure, *Micropaleontology*, 46(suppl. 1), 57-86.

857 Hottinger, L.C. (2006), The “face” of benthic foraminifera, *Bollettino della Società*
858 *Paleontologica Italiana*, 45, 75–89.

859 Ilyina, T., and R. E. Zeebe (2012), Detection and projection of carbonate dissolution in
860 the water column and deep-sea sediments due to ocean acidification,
861 *Geophysical Research Letters*, 39, L06606, doi:10.1029/2012GL051272.

862 Jennions, S. M., E. Thomas, D. N. Schmidt, D. J. Lunt, and A. Ridgwell (2015),
863 Changes in benthic ecosystems and ocean circulation in the Southeast Atlantic
864 across Eocene Thermal Maximum 2, *Paleoceanography*, 30, 1059-1077, doi:
865 10.1002/2015PA002821.

866 John, E. H., P. N. Pearson, H. K. Coxall, H. Birch, B. S. Wade, and G. L. Foster (2013),
867 Warm ocean processes and carbon cycling in the Eocene, *Philosophical*
868 *Transactions of The Royal Society A*, 371, doi:10.1098/rsta.2013.0099.

869 John, E. H., J. D. Wilson, P. N. Pearson, and A. Ridgwell (2014), Temperature-
870 dependent remineralization and carbon cycling in the warm Eocene oceans,
871 *Palaeogeography, Palaeoclimatology, Palaeoecology*, 413, 158-155.

872 Jorissen, F. J. (1999), Benthic foraminiferal successions across Late Quaternary
873 Mediterranean sapropels, *Marine Geology*, 153, 91-101.

874 Jorissen, F. J., H. C. Stigter, and J. G. V. Widmark (1995), A conceptual model
875 explaining benthic foraminiferal microhabitats, *Marine Micropaleontology*, 26,
876 3-15.

877 Jorissen, F. J., C. Fontanier, and E. Thomas (2007), Paleoceanographical proxies based
878 on deep-sea benthic foraminiferal assemblages characteristics, in *Proxies in Late*
879 *Cenozoic Paleoceanography: Part 2: Biological tracers and biomarkers*, edited
880 by C. Hillaire-Marcel, and A. Vernal, pp. 263-326, Elsevier, Amsterdam,
881 Netherlands.

882 Katz, M. E., D. R. Katz, J. D. Wright, K. G. Miller, D. K. Pak, N. J. Shackleton, and E.
883 Thomas (2003), Early Cenozoic benthic foraminiferal isotopes: Species
884 reliability and interspecies correction factors, *Paleoceanography*, 18, 1024,
885 doi:10.1029/2002PA000798.

886 Kelly, D. C., T. J. Bralower, J. C. Zachos, I. Premoli-Silva, and E. Thomas (1996),
887 Rapid diversification of planktonic foraminifera in the tropical Pacific (ODP Site
888 865) during the late Paleocene Thermal Maximum, *Geology*, 24, 423-426.

889 Kelly, D. C., T. J. Bralower, and J. C. Zachos, (1998), Evolutionary consequences of the
890 latest Paleocene thermal maximum for tropical planktonic foraminifera,
891 *Palaeogeography, Palaeoclimatology, Palaeoecology*, 141, 139–161.

892 Kelly, D. C., T. M. J. Nielsen, H. K. McCarren, J. C. Zachos, and U. Röhl (2010),
893 Spatiotemporal patterns of carbonate sedimentation in the South Atlantic:

894 Implications for carbon cycling during the Paleocene–Eocene thermal
895 maximum, *Palaeogeography, Palaeoclimatology, Palaeoecology*, 293(1-2), 30–
896 40.

897 Kelly, D. C., T. M. J. Nielsen, and S. A. Schellenberg (2012), Carbonate saturation
898 dynamics during the Paleocene–Eocene thermal maximum: Bathyal constraints
899 from ODP sites 689 and 690 in the Weddell Sea (South Atlantic), *Marine*
900 *Geology*, 303-306, 75–86.

901 Kennett, J. P., and L. D. Stott (1991), Abrupt deep-sea warming, palaeoceanographic
902 changes and benthic extinctions at the end of the Palaeocene, *Nature*, 353, 225-
903 229.

904 Korty, R. L., K. A. Emanuel, and J. R. Scott (2008), Tropical cyclone-induced upper-
905 ocean mixing and climate: application to equable climates, *Journal of Climate*,
906 21, 638-654.

907 Kossin, J. P., Emanuel, K. A., and Vecchi, G. A. (2014), The poleward migration of the
908 location of tropical cyclone maximum intensity. *Nature*, 509, 349-352

909 Kozdon, R., D. C. Kelly, N. T. Kita, J. H. Fournelle, and J. W. Valley (2011),
910 Planktonic foraminiferal oxygen isotope analysis by ion microprobe technique
911 suggests warm tropical sea surface temperatures during the Early Paleogene,
912 *Paleoceanography*, 26, PA3206, doi:10.1029/2010PA002056.

913 Kozdon, R., D. C. Kelly, K. Kitajima, A. Strickland, J. H. Fournelle, and J. W. Valley
914 (2013), In situ $\delta^{18}\text{O}$ and Mg/Ca analyses of diagenetic and planktic foraminiferal
915 calcite preserved in a deep-sea record of the Paleocene-Eocene thermal
916 maximum, *Paleoceanography*, 28(3), 517-528, doi:10.1002/palo.20048.

917 Kurtz, A. C., L. R. Kump, M. A. Arthur, J. C. Zachos, and A. Paytan (2003), Early
918 Cenozoic decoupling of the global carbon and sulfur cycles, *Paleoceanography*,
919 18(4), 1090, doi:10.1029/2003PA000908.

920 Kustanowich, S. (1962), A foraminiferal fauna from Capricorn Seamount, southwest
921 equatorial Pacific, *New Zealand Journal of Geology and Geophysics*, 5(3), 427-
922 434.

923 Lauretano, V., K. Littler, M. Polling, J. C. Zachos, and L. J. Lourens (2015), Frequency,
924 magnitude and character of hyperthermia; events at the onset of the early Eocene
925 Climatic Optimum, *Climate of the Past Discussions*, 11, 1795-1820.

926 Lavelle, W., and C. Mohn (2010), Motion, commotion, and biophysical connections at
927 deep ocean seamounts, *Oceanography*, 23(1), 91-103.

928 Leon-Rodriguez, L., and G. R. Dickens (2010), Constraints on ocean acidification
929 associated with rapid and massive carbon injections: The early Paleogene record
930 at ocean drilling program site 1215, equatorial Pacific Ocean, *Palaeogeography*,
931 *Palaeoclimatology, Palaeoecology*, 298, 409-420.

932 Littler, K., U. Röhl, T. Westerhold, and J. C. Zachos (2014), A high-resolution benthic
933 stable-isotope record for the South Atlantic: Implications for orbital-scale
934 changes in Late Paleocene–Early Eocene climate and carbon cycling, *Earth and
935 Planetary Science Letters*, 401, 18-30.

936 Loeblich, A. R. Jr., and H. Tappan (1987), *Foraminifera genera and their classification*,
937 Van Nostrand Reinhold Company Inc., New York.

938 Lourens, L. J., A. Suijs, D. Kroon, J. C. Zachos, E. Thomas, U. Röhl, J. Bowles, and I.
939 Raffi (2005), Astronomical pacing of late Palaeocene to early Eocene global
940 warming events, *Nature*, 435, 1083-1087.

941 Lunt, D. J., A. Ridgwell, A. Sluijs, J. C. Zachos, S. Hunter, and A. Haywood (2011), A
942 model for orbital pacing of methane hydrate destabilization during the
943 Paleogene, *Nature Geoscience*, 4, 775-778.

944 Lutze, G. F., and H. Thiel (1989), Epibenthic foraminifera from elevated microhabitats:
945 *Cibicidoides wuellerstorfi* and *Planulina ariminensis*, *Journal of Foraminiferal*
946 *Research*, 19(2), 153-158.

947 Ma, Z., E. Gray, E. Thomas, B. Murphy, J. C. Zachos, and A. Paytan (2014), Carbon
948 sequestration during the Paleocene-Eocene Thermal maximum by an efficient
949 biological pump, *Nature Geoscience*, 7, 382-388.

950 Mackensen, A., G. Schmied, J. Harloff, and M. Giese (1995), Deep-sea foraminifera in
951 the South Atlantic Ocean: Ecology and assemblage generation,
952 *Micropaleontology*, 41, 342-358.

953 Mancin, N., B. W. Hayward, I. Trattenero, M. Cobianchi, and C. Lupi (2013), Can the
954 morphology of deep-sea benthic foraminifera reveal what caused their extinction
955 during the mid-Pleistocene Climate Transition?, *Marine Micropaleontology*,
956 104, 53-70.

957 Martin, J. H., G. A. Knauer, D. M. Karl, and W. W. Broenkow (1987), VERTEX:
958 Carbon cycling in the north-east pacific, *Deep-Sea Research*, 34, 267-285.

959 Martini, E. (1971), Standard Tertiary and Quaternary calcareous nannoplankton
960 zonation, in *Proc. 2nd International Conference Planktonic Microfossils Roma*,
961 vol. 2, edited by A. Farinacci, pp. 739-785, Ed. Tecnosci., Rome.

962 McCarren, H., E. Thomas, T. Hasegawa, U. Röhl, and J. C. Zachos (2008), Depth-
963 dependency of the Paleocene-Eocene Carbon Isotope Excursion: Paired benthic
964 and terrestrial biomarker records (ODP Leg 208, Walvis Ridge), *Geochemistry*,
965 *Geophysics, Geosystems*, 9(10), Q10008, doi:10.1029/2008GC002116.

966 McClain, C. R. (2007), Seamounts: identity crisis or split personality?, *Journal of*
967 *Biogeography*, 34, 2001-2008.

968 McClain, C. R., L. Lundsten, M. Ream, J. Barry, and A. DeVogelaere (2009),
969 Endemicity, biogeography, composition and community structure on a
970 Northwest Pacific Seamount, *Plos One*, 4(1), e4141.

971 McInerney, F. A., and S. Wing (2011), The Paleocene-Eocene Thermal Maximum: a
972 perturbation of carbon cycle, climate, and biosphere with implications for the
973 future, *Annual Review of Earth Planetary Sciences*, 39, 489-516.

974 Mullineaux, L. S., and S. W. Mills (1997), A test of the larval retention hypothesis in
975 seamount-generated flows, *Deep-Sea Research I*, 44(5), 745-770.

976 Murray, J. W. (2001), The niche of benthic foraminifera, critical thresholds and proxies,
977 *Marine Micropaleontology*, 41, 1-7.

978 Nicolo, M. J., G. R. Dickens, C. J. Hollis, and J. C. Zachos (2007), Multiple early
979 Eocene hyperthermals: Their sedimentary expression on the New Zealand
980 continental margin and in the deep sea, *Geology*, 35(8), 699-702.

981 Nguyen, T. M. P., M. R. Petrizzo, and R. P. Speijer (2009), Experimental dissolution of
982 a fossil foraminiferal assemblage (Paleocene-Eocene Thermal Maximum,
983 Dababiya, Egypt): Implications for a paleoenvironmental reconstructions,
984 *Marine Micropaleontology*, 73, 241-258, doi:10.1016/j.marmicro.2009.10.005.

985 Nienstedt, J., and A. J. Arnold (1988), The distribution of benthic foraminifera on
986 seamounts near the East Pacific Rise, *Journal of Foraminiferal Research*, 18(3),
987 237-249.

988 Nisbet, E. G., S. M. Jones, J. Maclennan, G. Eagles, J. Moed, N. Warwick, S. Bekki, P.
989 Braesicke, J. A. Pyle, and C. M. R. Fowler (2009), Kick-starting ancient global
990 warming, *Nature geoscience*, 2, 156-159.

991 Nunes, F., and R. D. Norris (2006), Abrupt reversal in ocean overturning during the
992 Palaeocene/Eocene warm period, *Nature*, 439, 60-63.

993 Ohkushi, K., and H. Natori (2001), Living benthic foraminifera of the Hess Rise and
994 Suiko Seamount, central North Pacific, *Deep-Sea Research I*, 48, 1309-1324.

995 Ortiz, S., L. Alegret, A. Payros, X. Orue-Etxebarria, E. Apellaniz, and E. Molina
996 (2011), Distribution patterns of benthic foraminifera across the Ypresian-
997 Lutetian Gorrondatxe section, Northern Spain: response to sedimentary
998 disturbance, *Marine Micropaleontology*, 78, 1-13.

999 Pagani, M., N. Pedentchouk, M. Huber, A. Sluijs, S. Schouten, H. Brinkhuis, J. S.
1000 Sinninghe Damsté, G. R. Dickens, and Expedition 302 Scientists (2006), Arctic
1001 hydrology during global warming at the Palaeocene/Eocene thermal maximum,
1002 *Nature*, 442, 671–675.

1003 Pälike, H., et al. (2012), A Cenozoic record of the equatorial Pacific carbonate
1004 compensation depth, *Nature*, 488(7413), 609–614.

1005 Pälike, C., M. L. Delaney, and J. C. Zachos (2014), Deep-sea redox across the
1006 Paleocene-Eocene thermal maximum, *Geochemistry, Geophysics, Geosystems*,
1007 15(4), 1038–1053, doi:10.1002/2013GC005074.

1008 Pawlowski, J., J. Fahrni, B. Lecroq, D. Longet, N. Cornelius, L. Escoffier, T. Cedhagen,
1009 and A. J. Gooday (2007), Bipolar gene flow in deep-sea benthic foraminifera,
1010 *Molecular Ecology*, 16(19), 4089-4096.

1011 Payros, A., S. Ortiz, L. Alegret, X. Orue-Etxebarria, E. Apellaniz, and E. Molina
1012 (2012), An early Lutetian carbon-cycle perturbation: Insights from the
1013 Gorrondatxe section (western Pyrenees, Bay of Biscay), *Paleoceanography*,
1014 27(2), PA2213, doi:10.1029/2012PA002300.

1015 Pearson, P. N., P. W. Ditchfield, J. Singano, K. G. Harcourt-Brown, C. J. Nicholas, R.
1016 K. Olsson, N. J. Shackleton, and M. A. Hall (2001), Warm tropical sea surface
1017 temperatures in the Late Cretaceous and Eocene epochs, *Nature*, 413, 481–487.

1018 Pearson, P. N., B. E. van Dongen, C. J. Nicholas, R. D. Pancost, S. Schouten, J. M.
1019 Singano, and B. S. Wade (2007), Stable warm tropical climate through the
1020 Eocene Epoch, *Geology*, 35, 211-214.

1021 Penman, D. E., B. Hoenisch, R. E. Zeebe, E. Thomas, and J. C. Zachos (2014), Rapid
1022 and sustained surface ocean acidification during the Paleocene-Eocene Thermal
1023 maximum, *Paleoceanography*, 29(5), 357-369, doi:10.1002/2014PA002621.

1024 Röhl, U., T. Westerhold, S. Monechi, E. Thomas, J. C. Zachos, and B. Donner (2005),
1025 The third and final early Eocene Thermal Maximum: characteristic, timing, and
1026 mechanisms of the “X” event, *Geological Society of America Abstracts with*
1027 *Programs*, 37(7), 264.

1028 Sager, W. W., E. L. Winterer, J. V. Firth, et al. (1993), Site 865, in *Proceedings of the*
1029 *Ocean Drilling Program, Initial Reports*, vol. 143, edited by W. W. Sager et al.,
1030 pp. 111-180, College Station, Texas, Ocean Drilling Program.

1031 Samadi, S., L. Bontan, E. Macpherson, B. R. de Forges, and M. C. Boisselier (2006),
1032 Seamount endemism questioned by the geographic distribution and population
1033 genetic structure of marine invertebrates, *Marine Biology*, 149, 1463-1475.

1034 Schmiedl, G., A. Mitschele, S. Beck, K. C., Emeis, C. Hemleben, H. Schulz, M.
1035 Sperling, and S. Weldeab (2003), Benthic foraminiferal record of ecosystem
1036 variability in the eastern Mediterranean Sea during times of sapropel S₅ and S₆
1037 deposition, *Palaeogeography, Palaeoclimatology, Palaeoecology*, 190, 139-194.

1038 Schoenfeld, J. (2002), A new benthic foraminiferal proxy for near-bottom current
1039 velocities in the Gulf of Cadiz, northeastern Atlantic Ocean, *Deep-Sea Research*
1040 I, 49, 1853-1875.

1041 Sen Gupta, B. K., and M. L. Machain-Castillo (1993), Benthic foraminifera in oxygen-
1042 poor habitats, *Marine Micropaleontology*, 20, 3-4.

1043 Sexton, P. F., R. D. Norris, P. A. Wilson, H. Pälike, T. Westerhold, U. Röhl, C. T.
1044 Bolton, and S. Gibbs (2011), Eocene global warming events driven by
1045 ventilation of oceanic dissolved organic carbon, *Nature*, 471, 349-352.

1046 Shank, T. M. (2010), Seamounts: Deep-ocean laboratories of faunal connectivity,
1047 evolution and endemism, *Oceanography*, 23(1), 109-122.

1048 Sluijs, A., G. J. Bowen, H. Brinkhuis, L. J. Lourens, and E. Thomas (2007), The
1049 Paleocene-Eocene Thermal Maximum super greenhouse: biotic and geochemical
1050 signatures, age models and mechanisms of global change, in *Deep time*
1051 *perspectives on climate change: marrying the signal from computer models and*
1052 *biological proxies*, vol. 2, edited by M. Williams et al., pp. 323-349, The
1053 *Micropaleontological Society Special Publications and The Geological Society*,
1054 London.

1055 Sluijs, A., S. Schouten, T. H. Donders, P. L. Schoon, U. Röhl, G. Reichart, F. Sangiorgi,
1056 J. Kim, J. S. Sinninghe Damsté, and H. Brinkhuis (2009), Warm and wet
1057 conditions in the Arctic region during Eocene Thermal Maximum 2, *Nature*
1058 *Geoscience*, 2, 777-780.

1059 Sluijs, A., R. E. Zeebe, P. K. Bijl, and S. M. Bohaty (2013), A middle Eocene carbon
1060 cycle conundrum, *Nature Geoscience*, 6(6), 429-434.

1061 Smart, C. W., E. Thomas, and A. T. S. Ramsay (2007), Middle-late Miocene benthic
1062 foraminifera in a western Indian Ocean Depth Transect: paleoceanographic

1063 implications, *Palaeogeography, Palaeoclimatology, Palaeoecology*, 247, 402-
1064 420.

1065 Speijer, R. P., C. Scheibner, P. Stassen, and A. M. M. Morsi (2012), Response of
1066 marine ecosystems to deep-time global warming: A synthesis of biotic patterns
1067 across the Paleocene-Eocene thermal maximum (PETM), *Australian Journal of*
1068 *Earth Sciences*, 105, 6–16.

1069 Sriver, R. L., and M. Huber (2007), Observational evidence for an ocean heat pump
1070 induced by tropical cyclones, *Nature*, 447, 577-580.

1071 Stap, L., A. Sluijs, E. Thomas, and L. Lourens (2009), Patterns and magnitude of deep
1072 sea carbonate dissolution during Eocene Thermal Maximum 2 and H2, Walvis
1073 Ridge, southeastern Atlantic Ocean, *Paleoceanography*, 24(1), PA1211,
1074 doi:10.1029/2008PA001655.

1075 Stap, L., L. J. Lourens, E. Thomas, A. Sluijs, S. Bohaty, and J. C. Zachos (2010), High-
1076 resolution deep-sea carbon and oxygen isotope records of Eocene Thermal
1077 Maximum 2 and H2, *Geology*, 38(7), 607-610.

1078 Staudigel, H., A. A. P. Koopers, W. J. Lavelle, T. J. Pitcher, and T. M. Shank (2010),
1079 Defining the word “seamount”, *Oceanography*, 23(1), 20-21.

1080 Steineck, P. L., and E. Thomas (1996), The latest Paleocene crisis in the deep sea:
1081 Ostracode succession at Maud Rise, Southern Ocean, *Geology*, 24, 583-586.

1082 Svensen, H., S. Planke, A. Malthe-Sørenssen, B. Jam-tveit, R. Myklebust, T. R. Eidem,
1083 and S. S. Rey (2004), Release of methane from a volcanic basin as a mechanism
1084 for initial Eocene global warming, *Nature*, 429, 542–545.

1085 Svensen, H., S. Plankle, and F. Corfu (2010), Zircon dating ties NE Atlantic sill
1086 emplacement to initial Eocene global warming, *Journal of the Geological*
1087 *Society, London*, 167, 433-436.

1088 Storey, M., R. A. Duncan, and C. C. Jr. Swisher (2007), Paleocene-Eocene Thermal
1089 Maximum and the opening of the Northeast Atlantic, *Science*, 316, 587-589.

1090 Takeda, K., and K. Kaiho (2007), Faunal turnovers in central Pacific benthic
1091 foraminifera during the Paleocene-Eocene Thermal Maximum,
1092 *Palaeogeography, Palaeoclimatology, Palaeoecology*, 251, 175–197.

1093 Thistle, D., and L. A. Levin (1998), The effect of experimentally increased near-bottom
1094 flow on metazoan meiofauna at a deep-sea site, with comparison data on
1095 macrofauna, *Deep Sea Research I: Oceanographic Research Papers*, 45, 625-
1096 638.

1097 Thistle, D., L. A. Levin, A. J. Gooday, O. Pfannkuche, and P. J. D. Lambshead (1999),
1098 Physical reworking by near-bottom flow alters the metazoan meiofauna of
1099 Fieberling Guyot (northeast Pacific), *Deep Sea Research I: Oceanographic
1100 Research Papers*, 46, 2041-2052.

1101 Thomas, E. (1990), Late Cretaceous through Neogene deep-sea benthic foraminifers
1102 (Maud Rise, Weddell Sea, Antarctica), *Proceedings of the Ocean Drilling
1103 Program Scientific Results*, 113, 571-594.

1104 Thomas, E. (1998), The biogeography of the late Paleocene benthic foraminiferal
1105 extinction, in *Late Paleocene-Early Eocene Biotic and Climatic Events in the
1106 Marine and Terrestrial Records*, edited by M. P. Aubry et al., pp. 214-243,
1107 Columbia University Press, New York.

1108 Thomas, E. (2003), Extinction and food at the seafloor: A high-resolution benthic
1109 foraminiferal record across the Initial Eocene Thermal Maximum, Southern
1110 Ocean Site 690, in *Causes and Consequences of Globally Warm Climates in the
1111 Early Paleogene*, vol. 369, edited by S. L. Wing et al., pp. 319-332, Geological
1112 Society of America Special Paper, Boulder, Colorado.

- 1113 Thomas, E. (2007), Cenozoic mass extinctions in the deep sea: What perturbs the largest
1114 habitat on Earth?, in Large ecosystem perturbations: causes and consequences,
1115 vol. 424, edited by S. Monechi et al., pp. 1-23, Geological Society of America
1116 Special Paper, Boulder, Colorado.
- 1117 Thomas, E. and N. J. Shackleton (1996), The Paleocene-Eocene benthic foraminiferal
1118 extinction and stable isotope anomalies, in Correlation of the Early Paleogene in
1119 Northwest Europe, vol. 101, edited by R. W. O'B. Know et al., pp. 401-441,
1120 Geological Society Special Publication, London.
- 1121 Thomas, E., and J. C. Zachos (2000), Was the late Paleocene thermal maximum a
1122 unique event?, *Geologiska Foereningens i Stockholm Foerhandlingar*, 122, 169-
1123 170.
- 1124 Thomas, E., J. C. Zachos, and T. J. Bralower (2000), Deep-sea environments on a warm
1125 Earth: latest Paleocene-early Eocene, in *Warm climates in Earth history*, edited
1126 by B. Huber et al., pp. 132-160, Cambridge University Press, UK.
- 1127 Tjalsma, R. C., and G. P. Lohmann (1983), Paleocene-Eocene bathyal and abyssal
1128 benthic foraminifera from the Atlantic Ocean, *Micropaleontology Special*
1129 *Publication*, 4, 1-89.
- 1130 Tripathi, A., and H. Elderfield (2005), Deep-Sea Temperature and Circulation Changes at
1131 the Paleocene-Eocene Thermal Maximum, *Science*, 308, 1894-1898.
- 1132 van Morkhoven, F. P. C. M., W. A. Berggren, and A. S. Edwards (1986), Cenozoic
1133 cosmopolitan deep-water benthic foraminifera, *Bulletin des Centres de*
1134 *Recherches Exploration-Production Elf-Aquitaine, Memoir 11*, Pau, France.
- 1135 Webb, A. E., L. R. Leighton, S. A. Schellenberg, E. A. Landau, and E. Thomas (2009),
1136 Impact of Paleocene-Eocene global warming on microbenthic community

1137 structure: using rank-abundance curves to quantify ecological response,
1138 *Geology*, 37, 783-786.

1139 Westerhold, T., and U. Röhl (2013), Orbital pacing of Eocene climate during the Middle
1140 Eocene Climate Optimum and the chron C19r event: Missing link found in the
1141 tropical western Atlantic, *Geochemistry, Geophysics, Geosystems*, 14(11),
1142 4811-4825, doi:10.1002/ggge.20293.

1143 Wilson, C. D., and G. W. Boehlert (2004), Interaction of ocean currents and resident
1144 micronekton at a seamount in the central North Pacific, *Journal of Marine*
1145 *Science*, 50, 39-60.

1146 Winguth, A. M. E., E. Thomas, and C. Winguth (2012), Global decline in ocean
1147 ventilation, oxygenation, and productivity during the Paleocene-Eocene Thermal
1148 Maximum: Implications for the benthic extinction, *Geology*, 40(3), 263-266.

1149 Yamaguchi, T., and R. D. Norris (2012), Deep-sea ostracode turnovers through the
1150 Paleocene-Eocene thermal maximum in DSDP Site 401, Bay of Biscay, North
1151 Atlantic, *Marine Micropaleontology*, 86-87, 32-44.

1152 Yamaguchi, T., and D. Norris (2015), No place to retreat: Heavy extinction and delayed
1153 recovery on a Pacific guyot during the Paleocene-Eocene Thermal Maximum,
1154 *Geology*, 43(5), 443-446.

1155 Yasuhara, M., G. Hunt, T. M. Cronin, N. Hokanishi, H. Kawahata, A. Tsujimoto, and
1156 M. Ishitake (2012), Climatic forcing of Quaternary deep-sea benthic
1157 communities in the North Pacific Ocean, *Paleobiology*, 38, 162-179.

1158 Zachos, J., M. Pagani, L. Sloan, E. Thomas, and K. Billups (2001), Trends, rhythms,
1159 and aberrations in global climate 65 Ma to present, *Science*, 292, 686-693.

1160 Zachos, J. C., M. W. Wara, S. Bohaty, M. L. Delaney, M. R. Petrizzo, A. Brill, T. J.
1161 Bralower, and I. Premoli-Silva (2003), A transient rise in tropical sea surface

1162 temperature during the Paleocene-Eocene Thermal Maximum, *Science*, 302,
1163 1551-1554.

1164 Zachos, J. C., U. Röhl, S. A. Schellenberg, A. Sluijs, D. A. Hodell, D. C. Kelly, E.
1165 Thomas, M. Nicolo, I. Raffi, L. J. Lourens, H. McCarren, and D. Kroon (2005),
1166 Rapid acidification of the ocean during the Paleocene-Eocene Thermal
1167 Maximum, *Science*, 308, 1611-1615.

1168 Zachos, J. C., G. R. Dickens, and R. E. Zeebe (2008), An early Cenozoic perspective on
1169 greenhouse warming and carbon-cycle dynamics, *Nature*, 451, 279-283.

1170 Zachos, J. C., H. McCarren, B. Murphy, U. Röhl, and T. Westerhold (2010), Tempo and
1171 scale of late Paleocene and early Eocene carbon isotope cycles: implications for
1172 the origin of hyperthermals, *Earth and Planetary Science Letters*, 299, 242-249.

1173 Zhou, X., E. Thomas, R. E. M. Rickaby, A. M. E. Winguth, and Z. Lu (2014), I/Ca
1174 evidence for global upper ocean deoxygenation during the Paleocene-Eocene
1175 Thermal Maximum (PETM), *Paleoceanography*, 29(10), 964-975,
1176 doi:10.1002/2014PA002702.

1177

1178

1179

1180

1181

1182

1183

1184

1185

1186

1187 **Table 1.** Eocene hyperthermal events.

Hyperthermal Events	Age (Ma)	References
Eocene Thermal Maximum-2 (ETM2, also called ELMO or H1)	53.7	<i>Lourens et al.</i> , 2005; <i>Sluijs et al.</i> , 2009; <i>Galeotti et al.</i> , 2010; <i>Leon-Rodriguez and Dickens</i> , 2010; <i>Stap et al.</i> , 2009, 2010
H2	53.6	<i>Cramer et al.</i> , 2003; <i>Stap et al.</i> , 2009, 2010
I1	53.2	<i>Cramer et al.</i> , 2003; <i>Leon-Rodriguez and Dickens</i> , 2010
Eocene Thermal Maximum-3 (ETM3 or X event)	52.5	<i>Cramer et al.</i> , 2003; <i>Röhl et al.</i> , 2005; <i>Agnini et al.</i> , 2009; <i>Galeotti et al.</i> , 2010; <i>Leon-Rodriguez and Dickens</i> , 2010
C22r-H1 to H3	50-48.2	<i>Sexton et al.</i> , 2011
C21r-H6	47.44	<i>Sexton et al.</i> , 2011; <i>Payros et al.</i> , 2012
C19r	41.8	<i>Edgar et al.</i> , 2007

1188

1189

1190

1191

1192

1193

1194

1195

1196

1197

1198

1199

1200

1201

1202

1203

1204

1205

1206 **Table 2.** Benthic foraminifera mentioned in the text, including some of their ecological preferences and paleoenvironmental
 1207 implications.

Group	Selected species	Test	Life position	Ecological preferences/paleoenvironmental implications
Bolivinids s.s.	<i>Bolivinoides decoratus</i>	Calcareous	Infaunal	Abundant food supply and/or low oxygenation ^{a,b,c}
	<i>Tappanina selmensis</i>	Calcareous	Infaunal	Abundant food supply and/or low oxygenation ^{a,b,c}
Buliminids s.s.	<i>Bulimina semicostata</i>	Calcareous	Infaunal	High food environments ^{c,d}
	<i>Bulimina simplex</i>	Calcareous	Infaunal	High food environments ^{c,d}
	<i>Buliminella beaumonti</i>	Calcareous	Infaunal	High food environments ^{c,d}
	<i>Quadratobul. pyramidalis</i>	Calcareous	Infaunal	High food environments ^{c,d}
	<i>Siphogen. brevispinosa</i>	Calcareous	Infaunal	High food environments ^{c,d}
Buliminids s.l.	<i>Aragonia aragonensis</i>	Calcareous	Infaunal	Opportunistic, potential marker of hyperthermals ^{e,f,g}
	<i>Globocassid. subglobosa</i>	Calcareous	Infaunal	Oxic, pulsed food input, fresh phytodetritus ^{c,h}
	Pleurostomellids	Calcareous	Infaunal	High food supply ⁱ
	<i>Pyramidina rudita</i>	Calcareous	Infaunal	Opportunistic, high food supply ^{j,o}
Cylindrical taxa	<i>Stilostomella</i> spp.	Calcareous	Infaunal	Resistant to enhanced current activity ^o
	<i>Strictocostella</i> spp.	Calcareous	Infaunal	Resistant to enhanced current activity ^o
Uniserial lagenids	Nodosariids	Calcareous	Infaunal	High food supply ⁱ
	Abyssaminids	Calcareous	Infaunal	Oligotrophy, opportunistic ^k
	<i>Cibicidoides</i> spp.	Calcareous	Epifaunal	Increased bottom-current activity ^{i,o}
	<i>Gyroidinoides</i> spp.	Calcareous	Epifaunal	Opportunistic, meso-oligotrophic environments ^l
	Lenticulinids	Calcareous	Shallow infaunal	Resistant to dissolution ^m
	<i>Nuttallides truempyi</i>	Calcareous	Epifaunal	Oligotrophy, tolerant to corrosive waters ^b
	<i>Nuttallides umbonifera</i>	Calcareous	Epifaunal	Oligotrophy, tolerant to corrosive waters ^b
	<i>Oridorsalis umbonatus</i>	Calcareous	Infaunal	Oxic, low sustained flux of degraded organic matter ⁿ
	<i>Stens. beccariiformis</i>	Calcareous	Epifaunal	High food supply ^{d,j}

1208 ^aSen Gupta and Machain-Castillo [1993]; ^bThomas, [1998]; ^cJorissen et al., [2007]; ^dAlegret and Thomas [2009]; ^eSteineck and Thomas
 1209 [1996]; ^fAlegret et al. [2009a]; ^gOrtiz et al. [2011]; ^hSmart et al., [2007]; ⁱThomas et al., [2000]; ^jAlegret and Thomas, [2005]; ^kThomas,
 1210 [2007]; ^lSchmiedl et al., [2003]; ^mNguyen et al., [2009]; ⁿMackensen et al., [1995]; ^oThis study.

1211 **Figure captions**

1212 Figure 1. Palaeogeographic reconstruction at 55.5 Ma, modified from *Hay et al.* [1999],
1213 showing all sites mentioned in text, and cross-section of Allison Guyot (ODP Site 865),
1214 modified from *Sager et al.* [1993]. The arrows show a schematic diagram of the current
1215 system over seamounts, according to *Mullineaux and Mills* [1997].

1216

1217 Figure 2. $\delta^{13}\text{C}$ and $\delta^{18}\text{O}$ values in benthic foraminiferal species across the upper
1218 Paleocene – middle Eocene at ODP Site 865, shown with weight % Coarse Fraction
1219 (CF%), benthic foraminiferal accumulation rates (BFAR), diversity and heterogeneity
1220 indices, percentages of agglutinated taxa, infaunal-epifaunal morphogroups, cylindrical
1221 taxa, buliminids *s.l.*, buliminids *s.s.*, bolivinids *s.s.*, *Cibicidoides* spp. and *N. truempyi*.
1222 See Table S2 for genera included in each morphological group; calcareous/agglutinated
1223 genera are shown in Table S3, and infaunal/epifaunal species in Table S4. Stable
1224 isotope data from *Bralower et al.* [1995a, b] and *Katz et al.*, [2003]. Abbreviations:
1225 H(S)-Heterogeneity (Shannon-Weaver), *s.s.-sensu stricto*, *s.l. sensu lato*.

1226

1227 Figure 3. $\delta^{13}\text{C}$ and $\delta^{18}\text{O}$ values in benthic foraminiferal species across the PETM at the
1228 ODP Site 865. Percentages of agglutinated taxa, infaunal-epifaunal morphogroups,
1229 cylindrical taxa, buliminids *s.l.*, buliminids *s.s.* and bolivinids *s.s.* Relative abundance of
1230 selected benthic foraminiferal taxa and percentage of coarse fraction. Stable isotope data
1231 from *Bralower et al.* [1995a, b] and *Katz et al.*, [2003].

1232

1233 Figure 4. $\delta^{18}\text{O}$ values vs. weight percent coarse fraction (CF%), and coarse fraction vs.
1234 relative abundance of cylindrical taxa. Stable isotope data from *Bralower et al.* [1995a,
1235 b] and *Katz et al.*, [2003].

1236

1237 Figure 5. $\delta^{13}\text{C}$ vs. $\delta^{18}\text{O}$ values, relative abundance of *Cibicidoides* species vs. coarse
1238 fraction, BFARs vs. %buliminids, and % cylindrical taxa and % *N. truempyi* across the
1239 PETM interval. Stable isotope data from *Bralower et al.* [1995a, b] and *Katz et al.*,
1240 [2003].

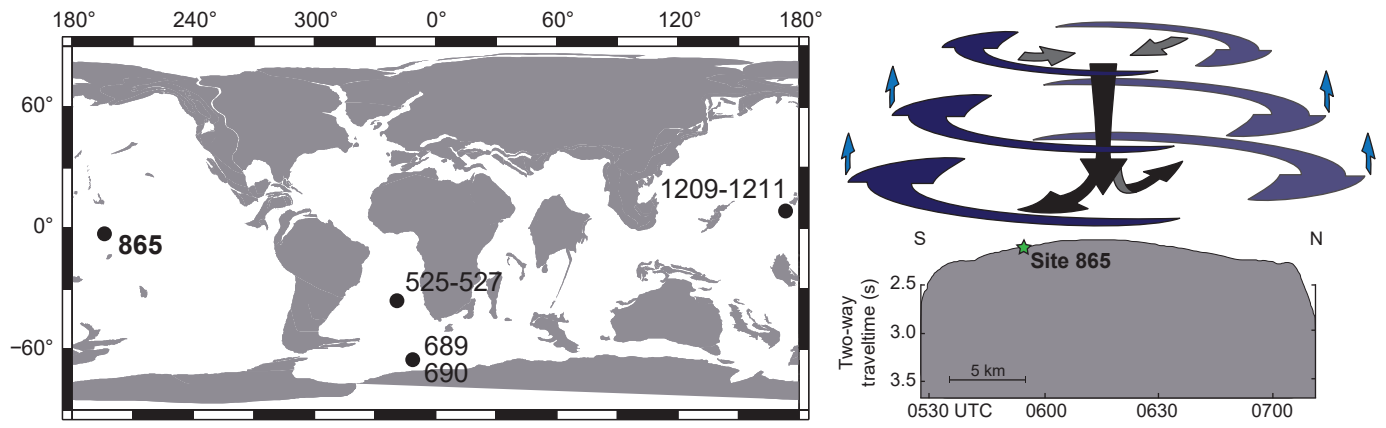
1241

1242 Figure 6. $\delta^{13}\text{C}$ and $\delta^{18}\text{O}$ values in benthic foraminiferal species across ETM3 event at
1243 ODP Site 865. Percentages of agglutinated taxa, infaunal-epifaunal morphogroups,
1244 cylindrical taxa, buliminids *s.l.*, buliminids *s.s.* and bolivinids *s.s.* Relative abundance of
1245 selected benthic foraminiferal taxa and percentage of coarse fraction. Stable isotope data
1246 from *Bralower et al.* [1995a, b] and *Katz et al.*, [2003].

1247

1248 Figure 7. Long-term evolution of inferred environmental parameters across the upper
1249 Paleocene to middle Eocene at ODP Site 865.

Figure 1



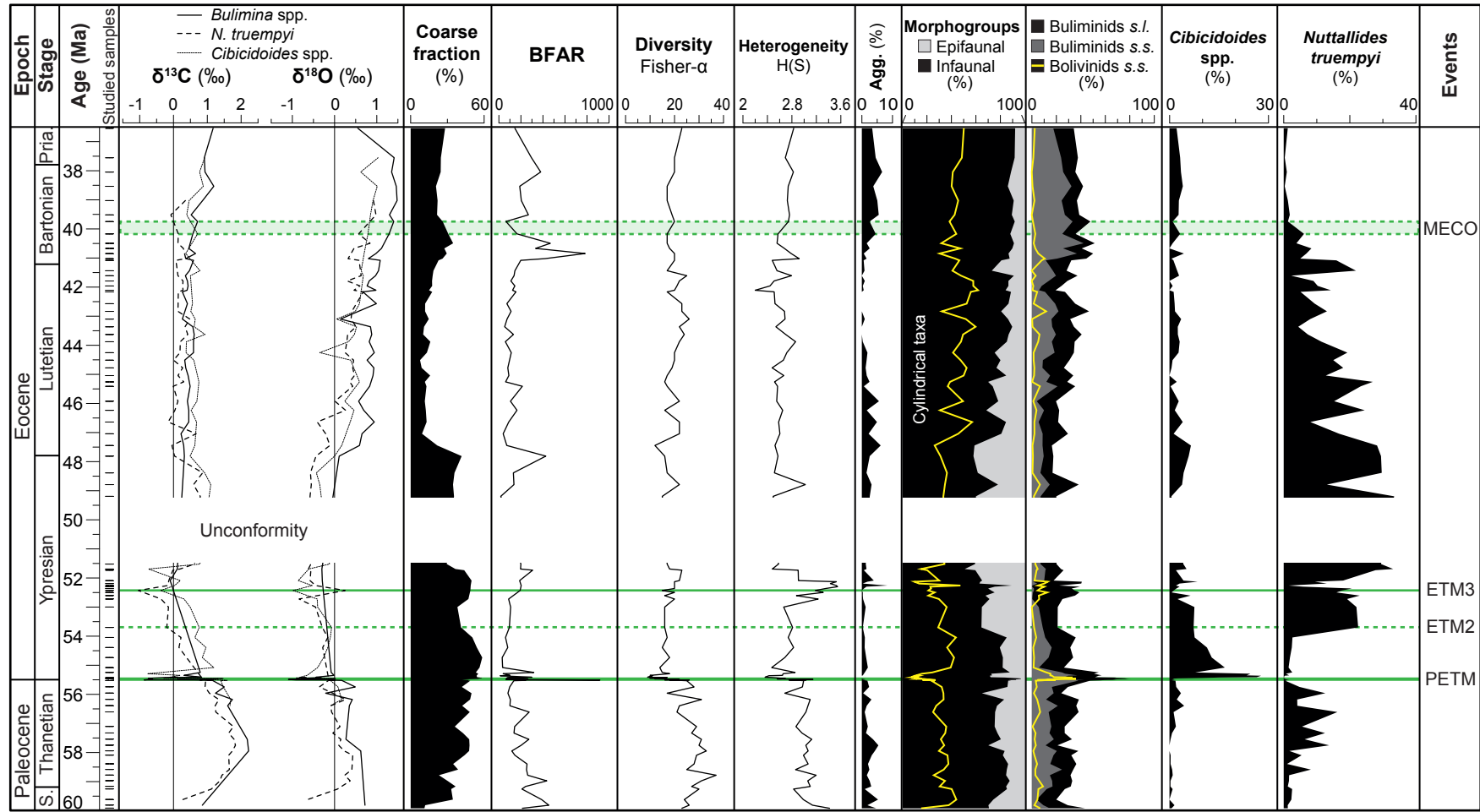


Figure 2

Figure 3

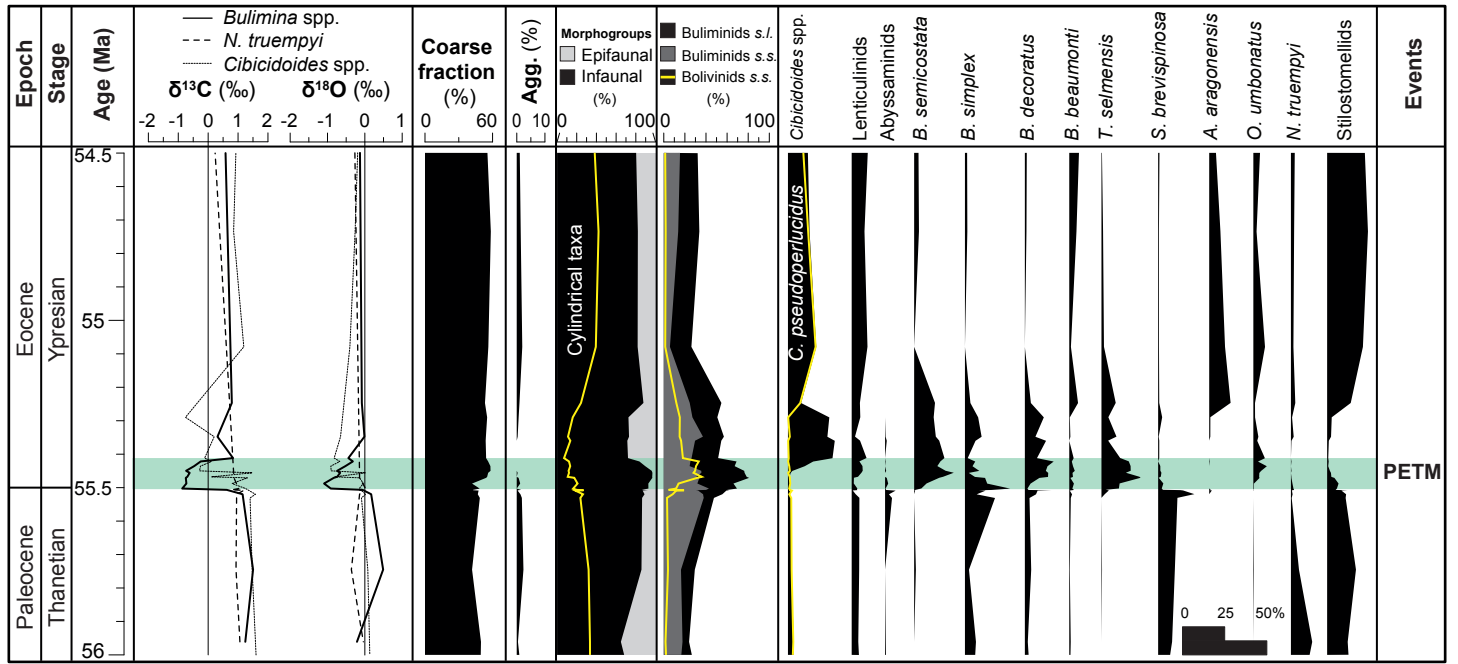


Figure 4

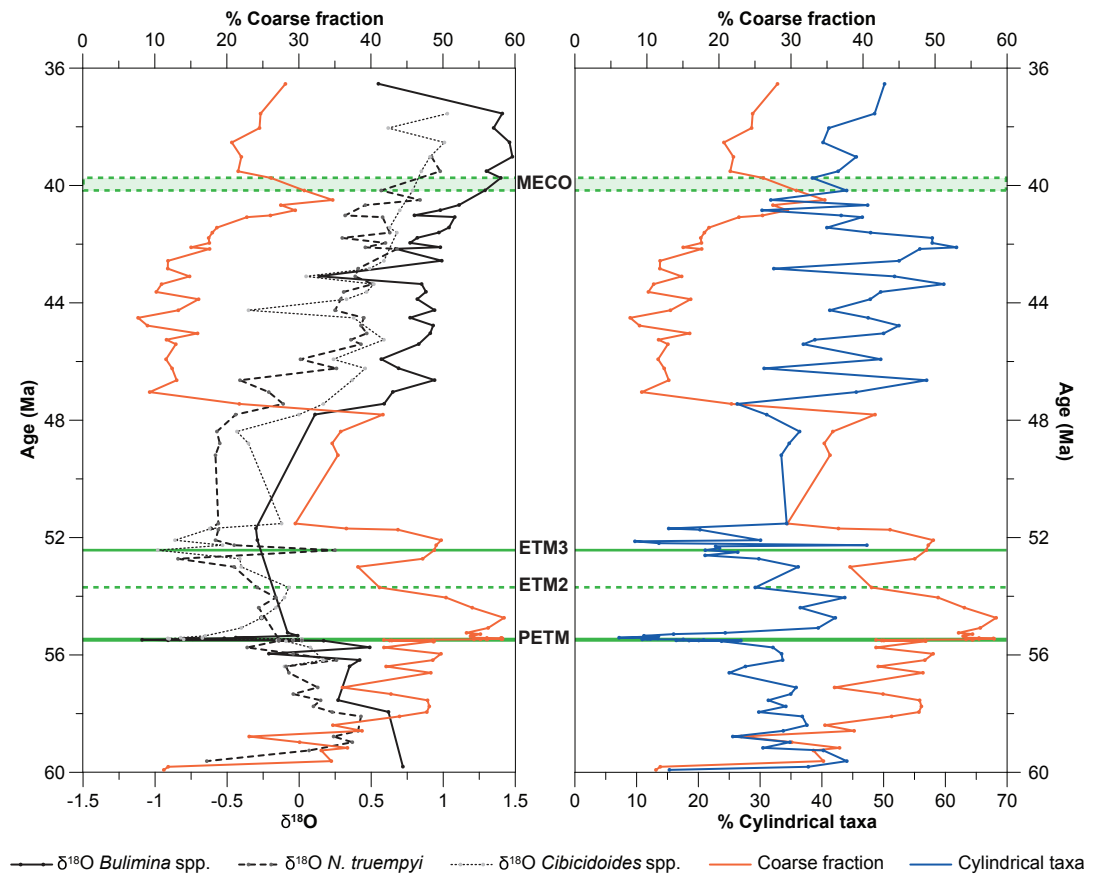


Figure 5

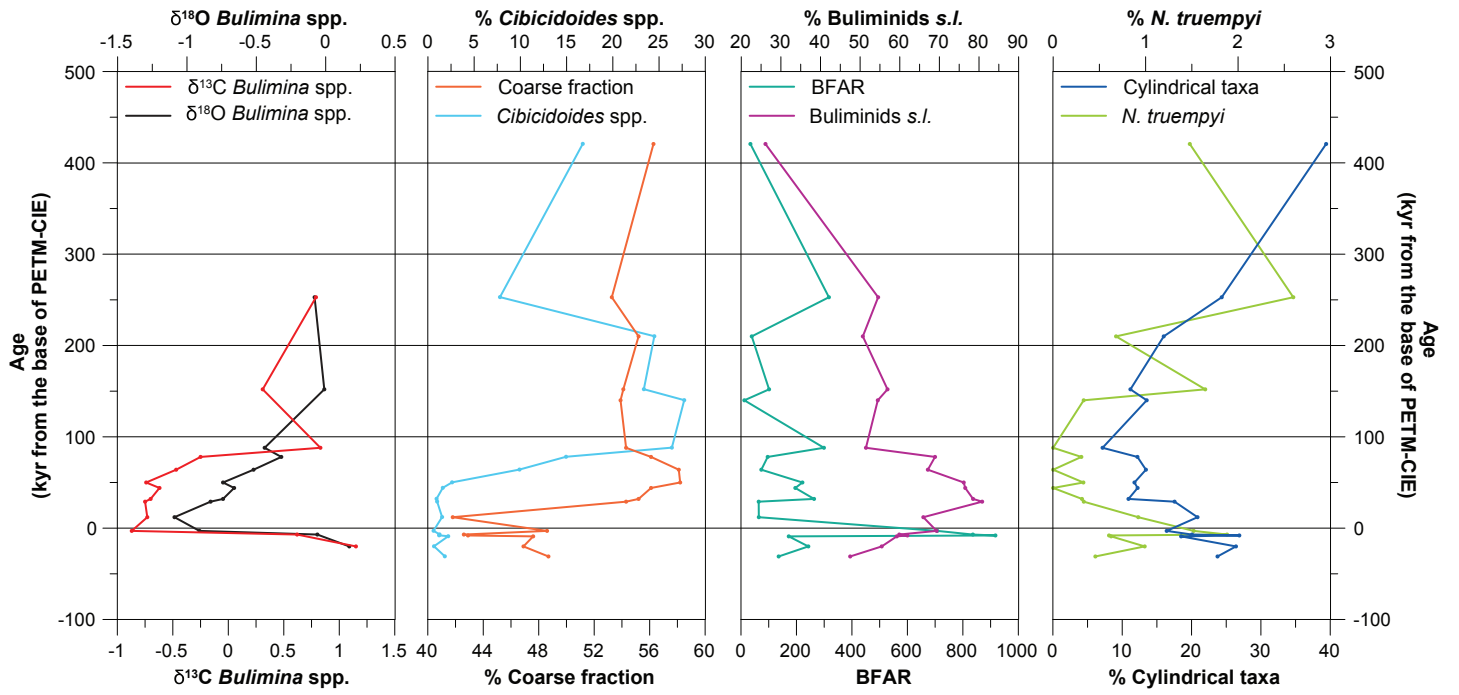


Figure 6

